Nuclear Instruments and Methods in Physics Research A 666 (2012) 173–196

Contents lists available at ScienceDirect

Nuclear Instruments and Methods in Physics Research A

journal homepage: www.elsevier.com/locate/nima

Review

Alignment systems in LHC general purpose detectors

J. Bensinger [a,*], T. Rodrigo [b]

[a] Brandeis University, Waltham, MA 02454, USA
[b] Instituto de Física de Cantabria IFCA/CSIC-UC, Santander, Spain

ARTICLE INFO

Available online 13 May 2011

Keywords:
Alignment
Optical alignment
CMS
ATLAS
LHC
Large hadron collider

ABSTRACT

Tracking systems in large multipurpose particle physics detectors are comprised of a large number of active elements designed, for precision measurement of particle trajectories. If detectors are to perform as designed a precise knowledge of the location of the different elements, with precision similar to the intrinsic detector resolution, is required. We will describe the design criteria and design considerations for optical alignment systems that achieve these goals. Issues discussed will include resolution discussions, integrating alignment with tracking detectors, geometric considerations, test beam activities, optical devices, calibration, and software analysis and validation procedures. We will describe the implementation of these ideas mainly in the CMS and ATLAS detectors operating at LHC.

Published by Elsevier B.V.

Contents

1. Introduction

Modern general-purpose collider experiments have several common features. They are motivated to look for new and unexpected physics phenomena in addition to precision measurements of known or expected phenomena. As such, they must detect and measure a variety of different objects with enough precision that any expected or possible new phenomena will not be missed. This leads to the requirement that measurements be made with the highest possible precision, with a particular emphasis on measurements of leptons, photons, and jets as they are directly produced in the interactions. This reasoning leads to some universal features of general-purpose collider experiments. These features comprise an inner, nondestructive tracking detector in a solenoidal magnetic field. The tracker is surrounded by a calorimeter, usually divided into electromagnetic and hadronic compartments. Surrounding the calorimeter is a muon spectrometer with either magnetic measurement or muon identification ability. In order to achieve precision of measurement capability required by the high energies involved, the size of detectors is quite large, and composed of many parts. The size of the detector and the magnitude of the magnetic field both drive the precision requirements of the tracking chambers. To achieve the precision expected for the detector, the components must be made

* Corresponding author.
E-mail address: bensinger@brandeis.edu (J. Bensinger).

0168-9002/$ - see front matter Published by Elsevier B.V.
doi:10.1016/j.nima.2011.04.058

precisely and their locations must be known precisely. As a general criterion, the expected alignment resolution should add no more than 20% to the intrinsic resolution of the measurement. This note will explore methods for measuring those locations, as they have been applied to the tracking systems of the ATLAS [1] and CMS [2] detectors operating at LHC.

The inner tracking system of CMS, with a size of 5.8 m in length and 2.5 m in diameter, surrounds the interaction point. It is composed of a pixel detector, consisting of 3 barrel layers at radii between 4.4 and 10.2 cm, followed by a silicon strip detector, made up of 10 layers extending up to a radius of 1.1 m. The system is completed by endcaps detectors, at each side of the barrel, which consist of 2 disks of pixel layers and 3 plus 9 disks of silicon strip detectors. In total there are 1440 pixel and 15.148 strip detector modules. The pixel cell has a size of $100\,\mu m \times 150\,\mu m$ in order to achieve similar resolution in the measured coordinates, r–ϕ and z. Depending on its proximity to the interaction point, the silicon detector uses different microstrip configurations ranging from 80 to 184 μm pitch. With this configuration and for a 100 GeV/c track, a resolution in transverse-momentum of about 1–2% is obtained in the central part (up to $\eta < 1.6$), beyond which the resolution degrades due to the reduced lever arm. The resolution in transverse impact parameter is about 10 μm for high momentum tracks.

Outer tracking detectors are dedicated to muon reconstruction and identification. The design of the CMS muon system is driven by the choice of its solenoid field. A 13 m length and 6 m inner diameter superconducting solenoid provides a 4 T magnetic field with a 12 Tm bending power. The return field is large enough to allow four stations of muon chambers integrated in the return yoke. The barrel region is instrumented with 4 stations of drift tube (DT) chambers, at different radius between 4 and 7 m, covering the pseudorapidity region $|\eta| < 1.2$. Each DT chamber consists of 8 layers of drift cell for the measurement of the r–ϕ coordinate, and a fourth layer (present only in the first 3 stations) to measure the z coordinate. In the two endcap regions, where the magnetic field is large and nonuniform, the muon system uses Cathode Strip Chambers (CSCs) covering up to 2.4 units in pseudorapidity. There are 4 stations of CSCs in each endcap, with chambers positioned perpendicular to the beam line and interspersed between the flux return disks. Each chamber has 6 measuring layers: the cathode strips run radially outward and provide a precision measurement in the r–ϕ bending plane. The anode wires run approximately perpendicular to the strips and provide measurements of η. To attain the desired precision in momentum measurement, the intrinsic spatial resolution of the muon chambers ranges from 55 to 120 μm, which translates to single layer resolutions between 125 and 500 μm. At low muon momentum, the stand-alone resolution is about 9%, while for high momentum, $\sim$1 TeV/c, the resolution varies between 15% and 40%, depending on pseudorapidity. A global momentum fit including the inner tracker information improves the momentum resolution by one order of magnitude, and for high momentum tracks, the achieved resolution is about 5%. A crucial property of the drift tubes and cathode strip chambers is to provide trigger capabilities with high efficiency and good background rejection. The requirement on the knowledge of chamber positioning is modest for trigger purposes, on the order of few millimeters, and gets more stringent for precise momentum measurement.

The ATLAS inner tracking system is composed of 3 layers of silicon pixel detectors, followed by the silicon strip detectors. That is surrounded by a Transition Radiation Tracker (TRT), a collection of xenon-filled straw tubes, which both measures tracks and detects transition radiation to help with electron identification. The coverage of the inner detector goes up to $|\eta| < 2.5$. The pixel detector has three cylindrical layers in the central region and two endcaps with three disks each. Outside the pixels, the Semi-Conductor Tracker (SCT) consists of silicon strip detectors and has 4 concentric central cylinders and the endcaps have 9 disks each. The straw tubes in the TRT are arranged in cylindrical layers in the central region and wheel like structures in the endcaps. The design resolution of the inner tracker is Delta(Pt)/$Pt = 0.005 \times Pt + 0.01$ and a transverse impact parameter of 10 μm for high momentum tracks.

The ATLAS muon spectrometer is based on a toroidal magnetic field provided by 3 large superconducting magnets arranged in 8-fold symmetry around the calorimeters. The barrel and two endcap toroids provide a toroidal magnetic field of approximately 0.5 T in the barrel and 1 T in the endcaps. These magnets provide a measurement that is essentially orthogonal to that of the inner detector. The muon spectrometer is designed to have resolution of 10% for muons having 1 TeV/c transverse-momentum. The muon system of the ATLAS detector, with a coverage of 2.7 in pseudorapidity, contains about 1200 precision tracking chambers ranging in size between 1 m × 1 m and 2 m × 6 m, complemented by a system of trigger chambers, which provide second coordinate information. The muon system is divided into 16 sectors, large and small, with the small sectors in the regions of the barrel toroid coils. The tracking technology uses high-pressure drift tubes and CSC for the high occupancy regions in the endcaps. There are approximately 300,000 tubes in the ATLAS muon system. With the available magnetic field and detector dimensions, this corresponds to a sagitta of 500 μm in the central (barrel) part of the detector, increasing to 1 mm in the forward (endcap) region. The 80 μm resolution of each drift tube and the number of tubes in a measurement lead to a sagitta resolution of 40 μm. The placement of chambers, with their attached alignment devices, in the muon spectrometer is typically 5 mm and 2 mrad with respect to their nominal positions. The alignment system is expected to improve on the knowledge of this position by more than 2 orders of magnitude. The size of the chambers, up to 6 m in the longest direction, is also of concern, as the chambers themselves may not be stable to the required precision.

The very large size of these detectors (see Figs. 1 and 2) – ATLAS is 25 m in diameter and 43 m along the collider beam – means that the measurement systems are made of a large numbers of components. Table 1 summarizes the main features of the tracking detector for ATLAS and CMS. To achieve the required measurement resolution the alignment system for the muon chambers must determine the location of each active detector to an accuracy of 30–40 μm, in the case of the ATLAS muon spectrometer, and about 100 μm for CMS. As long-term stability cannot be guaranteed at this precision, the alignment system must work continuously and stably over many years without drift or loss of resolution.

Precision measurement requires stringent quality control during the construction and assembly of the different detector units. Construction quality control is complemented with specific survey measurements [3] during the assembly phase of the individual detectors, as well as of the whole detector. Typical precision of survey ranges from few tens of microns to few millimeters, depending on the reference frame used. For the local measurements of small objects, a precision of about 30–50 μm can be reached. During detector assembly, the positioning of the subdetector units, e.g. muon chambers, are surveyed first with respect to the big detector structures, wheels or disks, with a precision of few hundreds of microns. Finally, using reference tragets on the cavern walls, the big structures are positioned with respect to the machine elements with a precision of few millimeters. This last step provides an initial geometry of the whole detector using an absolute reference in space and related to the machine elements and therefore with the beam line. It represents

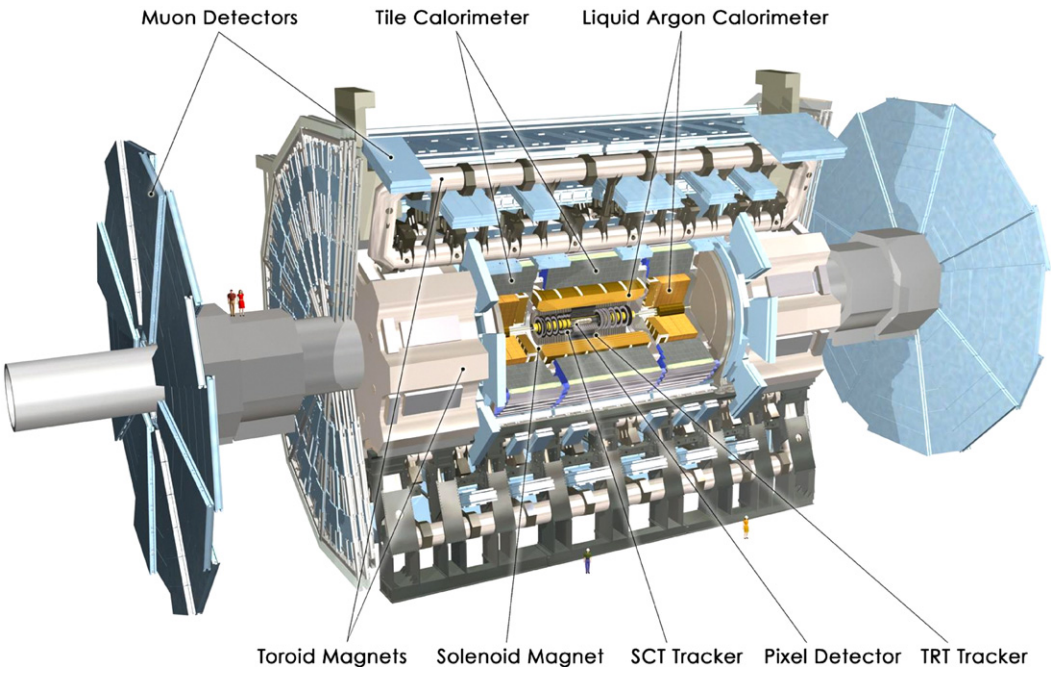

Fig. 1. Schematic view of the ATLAS detector with the different subsystems.

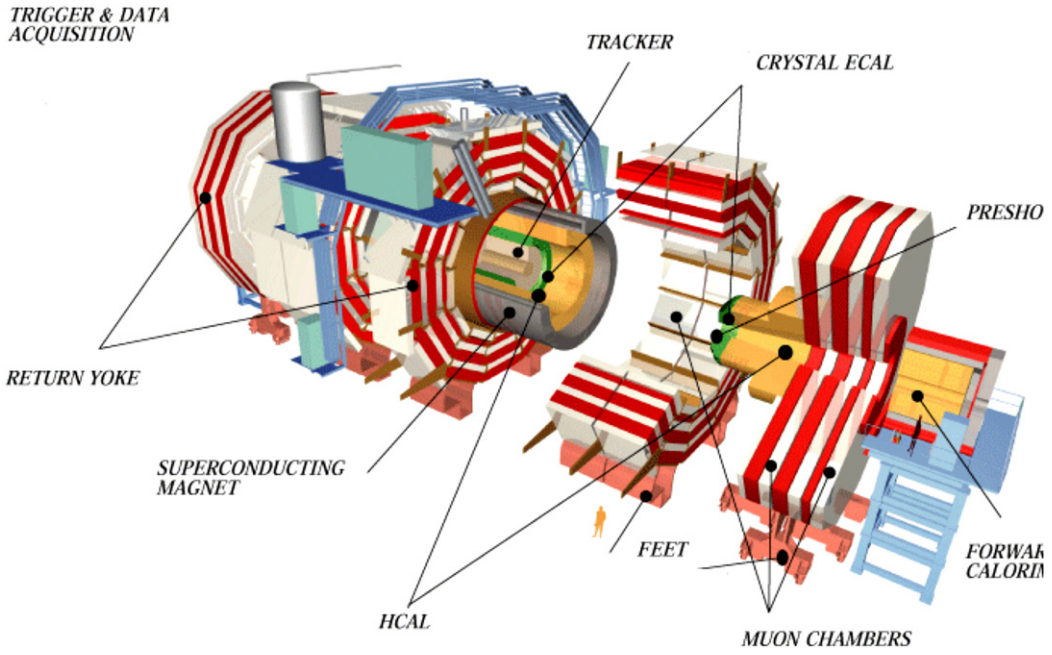

Fig. 2. Schematic view of the CMS detector, showing in an open configuration of the detector the different subsystems.

the best as-built detector information before further alignment, optical or track-based, measurements can be performed.

For both CMS and ATLAS, systems of optical, mechanical, and temperature sensors have been developed to detect chamber movement during operation and provide current chamber positions to the data analysis programs. These systems monitor chamber locations on a time scale ranging from hours to years, and are an essential ingredient in achieving the design goals of the experiments.

Future large general purpose experiments will have complicated tracking systems, in particular the muon system, which will be made of order 10^3 chambers. As the size and the complexity of the detectors grow, track-based alignment systems become more difficult and take a long time to achieve the desired accuracy. An alignment system that is fully operational at the beginning of data taking is essential to be able to make use of the data immediately. The goal of this paper is to provide the builders of future experiments the benefit of our experience building the alignment systems of CMS and ATLAS, rather than providing a complete description of these systems. We will demonstrate through examples that such a system, adequate for the detector design resolution, is possible. We will detail how CMS and ATLAS tried to

Table 1
Number of active tracking detectors in ATLAS and CMS [34].

Inner silicon tracking detectors						
	Volume (m^3)	Pixel layers	Resolution (μm)	Si-strip layers	Resolution (μm)	Channels (pixel+strips)
ATLAS	4.5	3	10×150	4–9	17×580	80M+6.3M
CMS	37.5	2–3	15–20	9–10	23–53	66M+9.3M
Muon spectrometers						
	Volume (m^3)	Stations	Resolution (μm)	Layers/station	Precision chambers	Readout channels
ATLAS	10,000	3	30–40	4–8	1182	385,000
CMS	2500	4	55–120	6–12	790	580,000

solve problems, and will provide some lessons learned for future developments.

2. System design considerations

Traditionally, the task of aligning tracking detectors in particle physics experiments has been accomplished mainly with the help of offline algorithms based on tracks (cosmic or collision tracks) traversing the detector. The stringent demands on spatial resolution of the active detector elements needed to satisfy the LHC physics goals, together with the large size of the detectors, were the main motivation for the development and implementation of large and complex opto-mechanical systems able to provide an active monitoring of the detector elements locations in a continuous mode and with high level of precision.

The task of these opto-mechanical alignment systems is to provide a redundant and independent measurement of the detector geometry, based on an internal light-based reference system that is not affected by systematic uncertainties that could be present in the standard track-based alignment approaches. Opto-mechanical alignment systems also provide a time-dependent monitoring of the detector stability, which allows establishing periods of validity for a given set of geometrical constants to be used in data processing and event reconstruction. In the design phase, uncertainties in the time scale of stability dictated a cycle time as fast as possible, typically a few tens of minutes.

It must be noted that although alignment generally means the active adjustment of an object with respect to others or to a static orientation, in the context of particle detectors, alignment is understood as the monitoring of the absolute space coordinates of an object and the changes in time of its location. Monitoring of the spatial positions of the detector elements among them allows two different approaches: absolute or relative measurements. Relative measurements, with respect to a given initial position, inform about time dependence variations but provide no information on the location of those elements in space. In this case, the initial position must be provided by other means, either external survey or track-based alignment algorithms. Instead, absolute position measurements provide the actual location in space of the monitored elements, and do not require extra source of information. Both ATLAS and CMS have chosen for their alignment systems this second approach. This guarantees that the alignment systems can be switched on/off without loss of precision.

In order to measure the geometry of the detector we need to know

- the position of individual active elements within a given subdetector,
- the position of the various subdetectors with respect to each other, and
- the position of the experiment with respect to the beam.

While the two first tasks are the aim of the alignment systems described here, the latter is generally reserved for the track-based alignment scheme. Track reconstruction and vertex fitting in the inner tracker detectors provide the global positioning of the detector with respect to the beam line.

Uncertainties contributing to the overall detector resolution result from multiple scattering effects, the knowledge of the magnetic field and material budget, the intrinsic detector resolution, and the knowledge of the geometrical position of the active detectors along the measured coordinates or alignment uncertainties. Assuming that all uncertainties due to the knowledge of magnetic field and material budget are under control, the measurement resolution for low momentum tracks is dominated by the error due to multiple scattering, while for high momentum tracks it will be limited by the intrinsic detector resolution. At the design phase, the intrinsic detector resolution is set to match the desired ultimate performance for high momentum tracks, while the alignment uncertainties are expected not to degrade the measurement precision by more than 20%. Therefore, to make full use of the detector elements resolution, their absolute position in space has to be determined with a similar level of precision.

Alignment requirements of the position measurement precision, for each space coordinate, are determined by the overall detector performance for high momentum tracks. The system layout is in turn defined by the momentum measurement strategy specific to each detector concept and the actual geometry of the detector. Other important design considerations include the expected range of motions, which will define the dynamic range of the system, its rate, and finally the environmental operating conditions that in the case of LHC detectors are mainly characterized by the tight spatial constraints imposed to maintain the desired detector hermeticity, the limited accessibility to the system components (and therefore limited maintenance capability), the exposure of the system components to strong magnetic fields, and exposure to high radiation doses over the foreseen period of operation.

2.1. Alignment strategy of inner tracking detectors

Inner tracking detectors are composed of a large number of position-sensitive elements that have intrinsic resolutions typically of the order of 10–30 μm. The overall strategy for the alignment of the inner detectors relies heavily on track-based offline alignment algorithms complemented by mechanical or optical monitoring information, known engineering tolerances, and rigidity of the support structures. A detailed review of track-

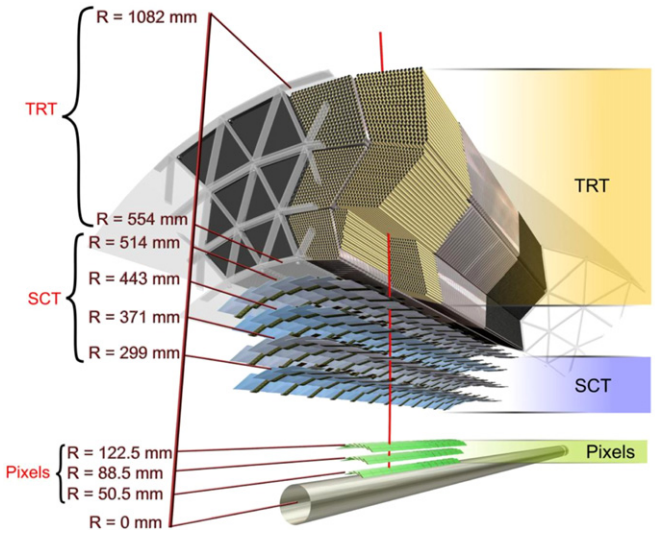

Fig. 3. Cutaway view of the ATLAS inner detector. The detector is contained in the 2 T solenoidal magnetic field. Shown here is only the barrel region of the detectors. Each detector has two endcaps organized as planar disks.

based alignment algorithms used in LHC detectors is given in Ref. [4]. In what follows, we concentrate on the description of the ATLAS and CMS inner tracking detectors.

The ATLAS inner detector is shown in Fig. 3. It is designed to full azimuthal coverage, and pseudorapidity coverage between ± 2.5 and a momentum resolution of Delta(Pt)/Pt=0.005 × Pt+0.01. The pixels are in 3 layers and provide 3 hit points on tracks. There are more than ~80 million readout channels of pixels typically 50 μm × 400 μm. Pulse height is measured by a time-over-threshold technique. The Semi-Conductor Tracker (SCT) consists of 4088 modules of silicon strip detectors. Sensors are glued back-to-back with a stereo angle of 40 mrad to provide space point. The total number of channels is ~6.3 million. Typically the SCT provides 8 strip hits or 4 space points on each track. Outside the SCT is the Transition Radiation Tracker (TRT). This device has ~300,000 proportional drift tubes (straws), 4 mm in diameter each. In the barrel, tracks typically cross more than 30 straws. In addition to track measurements, the TRT detects transition from polypropylene fibers in the barrel region and foils in the endcap regions.

The requirement that alignment degrades the resolution by no more than 20% means that the silicon pixels must be aligned to 7 μm and the silicon strips must be aligned to 12 μm in the r–ϕ direction. Along the beam line, the precision requirement is several tens of microns. The TRT alignment precision is required to be several tens of microns. The alignment is specified by the 3 translation and 3 rotation parameters. The alignment of the inner detector is track-based and determined by a χ^2 minimization of the residual between the measured track and the fitted track calculated with respect to the alignment parameters. For operational reasons, the TRTs were aligned after the pixels and SCT were aligned. Approximate factorization is used; aligning the modules with respect to each other, while ignoring deformation within the modules themselves. First, the largest structures (barrels and endcaps) are aligned, for which the largest misalignments are expected and the smallest statistics are needed. Afterward, additional degrees of freedom (barrel layers and endcap wheels) are added to compensate for the expected distortion given by the construction of the components. At the next step, the pixel staves (and an assumed stave structure for the SCT) were each aligned with the usual 6 degrees of freedom. After that, the individual modules of each stave were aligned using just 2 degrees of freedom consistent with the bowing of the staves. Because cosmic rays are not well distributed, especially in the endcaps, both cosmic ray and collision data were used for this alignment. The TRT was aligned after the pixel and SCT parts of the tracker were aligned. The first step of the TRT alignment was to perform the first level alignment with respect to the silicon. Because the TRT does not measure the position of hits along the straw, the translation along the wires was not aligned in the barrel. In the second stage, the TRT barrel was aligned internally, both for cosmic ray data taking periods with and without solenoid field. The corrections for both types of cosmic ray data were found compatible. Since the geometrical acceptance of the TRT for cosmic ray tracks is large, as compared to that of the silicon subsystem, the TRT stand-alone tracks were used to achieve high statistics for the internal alignment. The resolutions using these alignment constants are compatible with the Monte Carlo predictions for well aligned detectors. These procedures are more fully described in Ref. [5].

Moreover, interferometric measurements, described in Section 3.3, of the structural stability of the SCT are also performed. A survey system is built based on large number of simultaneous 1D interferometer measurement of absolute distances between selected points in the detector combined into an over constrained 3D geodesic network, thus allowing the computation of the positions in 3 dimensions. The geodesic grid of length measurements between nodes attached to the ATLAS SCT support structure consists of 842 lines lengths. One example for the barrel is shown in Section 3.3, Fig. 29. This system measures the mechanical stability of the ID support structure. These measurements are not yet integrated in the global strategy of the inner tracking system.

As shown in Fig. 4, the 15,148 modules of the CMS Silicon Strip tracker are organized in independent subsystems: Inner Barrel (TIB), Outer Barrel (TOB), 2 Endcap (TEC) disks, and 2 Inner Disks (TID). The barrel part is composed of 10 layers while in each inner and outer endcap there are 3 and 9 disks, respectively. Furthermore, the detector is instrumented with a dedicated optical system that is well integrated in the active detector elements, also shown in Fig. 4.

As with ATLAS, CMS bases the alignment of the inner tracker detector on track-based approaches. Two different statistical methods [5] have been adapted to specificities of the full silicon tracker detector of CMS: a local iterative algorithm, Hits and Impact Points (HIPs); and a global alignment algorithm, Millepede II. The strength of the global method is solving effectively the global correlations. The strengths of the local method are that the same track fit is used as in the standard CMS reconstruction, and that survey information can easily be incorporated thus allowing for alignment with more degrees of freedom. A first attempt of alignment, as described in Ref. [6], uses more than 3 million cosmic ray charged particles, with additional information from optical surveys. The positions of the modules are determined with respect to cosmic ray trajectories to a precision of 3–4 μm RMS in the barrel and 3–14 μm RMS in the endcaps in the most sensitive coordinate, close to the design values. The results have been validated by several methods, including the Laser Alignment System (LAS) [7], and compared with predictions obtained from the simulation.

The Laser Alignment System uses a set of 40 infrared laser beams (lambda=1075 nm). The light is detected directly on the silicon sensors, and therefore provides an excellent position resolution with respect to the active sensitive area. The LAS allows measuring the relative positions of the TIB, TOB, and of the TEC disks, but neither the TID nor the Pixel Tracker are included into the LAS layout. The aim of the LAS is to determine the global Strip Tracker structure position and orientation relative to each other with a precision of about 100 μm, which is necessary for track pattern recognition and for the High Level Trigger. It does not attempt to provide alignment parameters for

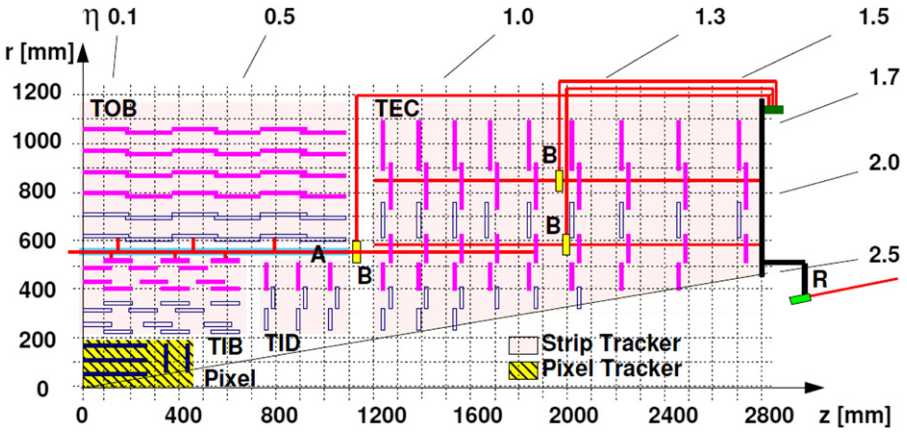

Fig. 4. Quarter of the CMS silicon tracker in an rz view. Single-sided silicon strip module positions are indicated as solid light (purple) lines, double-sided strip modules as open (blue) lines, and pixel modules as solid dark (blue) lines. Also shown are the paths of the laser rays (R), the beam splitters (B), and the alignment tubes (A) of the Laser Alignment System [7]. (For interpretation of the references to color in this figure legend, the reader is referred to the web version of this article.)

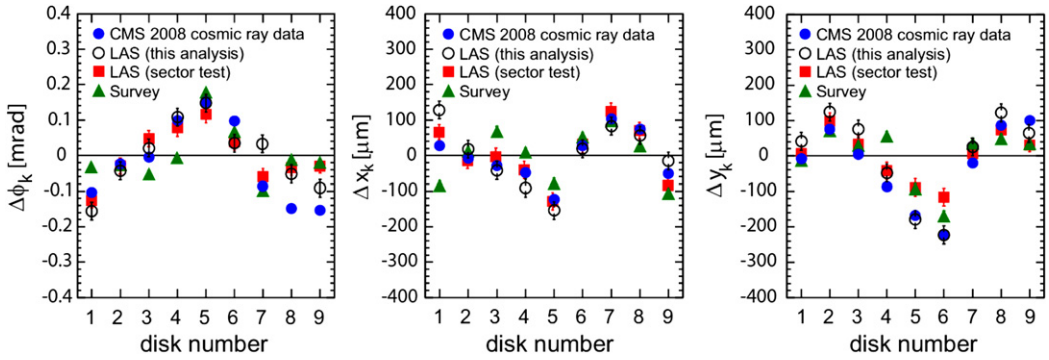

Fig. 5. The three alignment parameters for positive z TEC disks measured using cosmic ray data (solid blue circles), by the LAS in the analysis of the 2008 data [7] (open black circles), during the LAS sector test [33] (red squares), and by optical survey (green triangles): rotation around global z (left) and translations in global x (middle) and in global y (right). (For interpretation of the references to color in this figure legend, the reader is referred to the web version of this article.)

individual modules. Furthermore, the system is able to monitor relative positions with a precision of about 10 μm on a continuous mode and with a frequency of a few seconds. The data acquisition has been designed to allow LAS measurement during normal data taking such that variations on short time-scales can be followed. The geometrical layout of the LAS system is shown in Fig. 4.

Although the LAS system has not been fully exploited up to this writing, the available data have been used to calculate the relative positions of the TEC disks, and have been compared with other set of data from different analysis. The results are shown in Fig. 5.

ATLAS and CMS have chosen different concepts in the design of the optical systems. Due to the large number of active detector units, none of the optical systems attempts to monitor the entire detector by external optical means. In ATLAS, the stability of the support structures is monitored independently. The system is designed to measure absolute position coordinates of the structures, while the relation to the active detector units (silicon modules) is provided by precise construction and assembly measurements. In contrast, CMS monitors the relative position of the different detector parts, using a set of selected active units as alignment devices and thus avoiding as much as possible further mechanical transfers between measurements. At this writing, the optical systems are still in their commissioning phase and none of the concepts have yet been exploited to its full strength. A deep analysis of weakness and strengths of the present concept implementations will be useful for the design of future inner tracker detector optical alignment systems.

2.2. Alignment of muon detectors

The muon spectrometer is the outermost part of the detector. Thus the largest part, by volume, of the detector, with active measurement elements distributed throughout this large volume. Its geometry and the needed intrinsic detector resolution are determined by the choice made for the magnetic field, which in turn defines the momentum measurement strategy. Two possible options are present in the LHC experiments. The muon Pt is measured in ATLAS with an inner detector solenoid and a set of three toroidal air-core magnets for the muon, while in CMS the magnetic field for the muon system is provided by the solenoid return field inside the magnetized iron. The final performances in terms of muon momentum resolution are similar, the measurement is determined in both detectors from the inner tracker up to ~100 GeV/c (ATLAS) and ~200 GeV/c (CMS) and by combining muon and tracker data above these Pt values. Fig. 6 shows the CMS design performance on muon transverse-momentum resolution, and Fig. 7 shows the contributions to the resolution for muon momentum measurements in the ATLAS detector.

The design of the ATLAS muon alignment system is a hierarchy with three levels.

- At the first level, the shape, i.e. deformation and expansion, of each individual chamber is determined from the measurements of the 4 RASNIK (Red Alignment system of NIKHEF) [7] monitors (see Section 3.1) and temperature sensors built into the individual chambers.

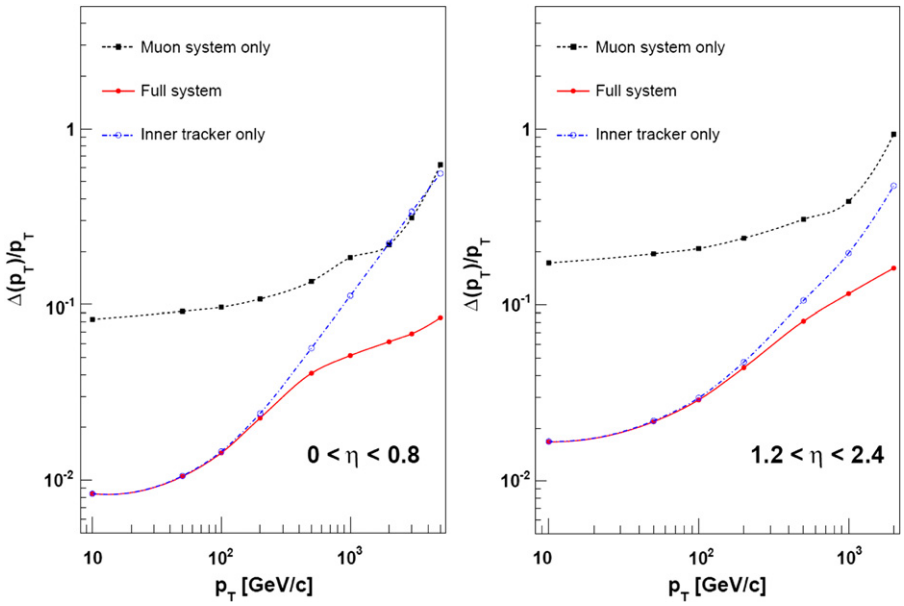

Fig. 6. CMS muon transverse-momentum resolution as a function of the transverse-momentum (*Pt*) using the muon system only, the inner tracking only, and both. Left panel: $|\eta| < 0{:}8$, right panel: $1{:}2 < |\eta| < 2{:}4$ [2].

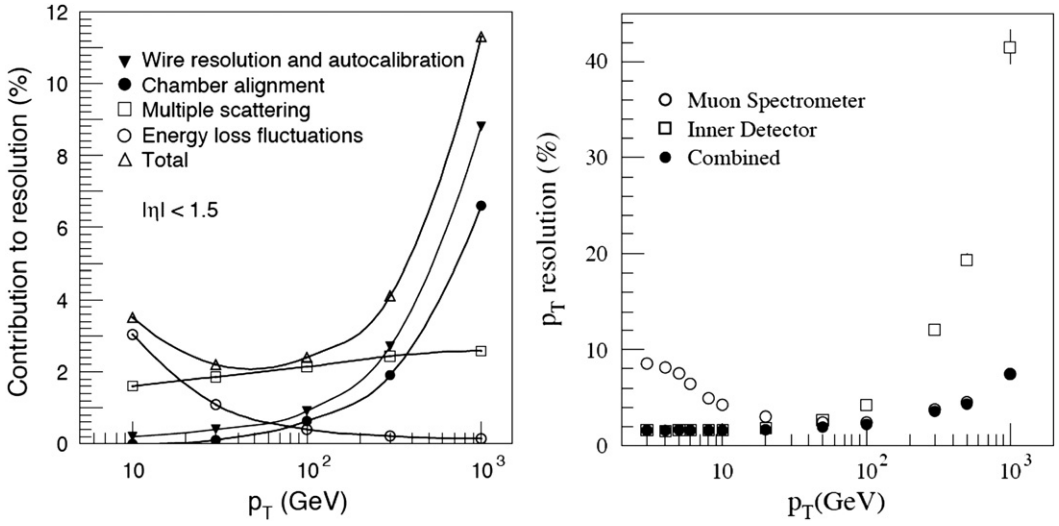

Fig. 7. ATLAS muon spectrometer resolution. The plot on the left shows the contribution to the momentum resolution from various sources. The plot on the right shows the combined resolution using both the inner detector and the muon spectrometer.

- In the endcap, the alignment bars determine the precise grid location, which measure their individual shapes and their positions with respect to each other using the measurements of a CCD optical based system (BCAMs, see Section 3.2) mounted on them. The assembly precision of the muon system was estimated at a few mm, so all sensors had to have a dynamic range of at least ± 10 mm.
- At the third level, chamber positions are determined. In the endcap, the positions of MDT chambers, measured in pairs, with respect to the nearest alignment bars are derived from the measurements by sensors located on the alignment bars and on the chambers.

The steps as listed above are more appropriate for the endcap, the sequence for the barrel is

- At the second level, in the barrel, an array of sensors locates the chambers of a given layer (axial–paraxial) in the large sectors supplemented by an optical connection to track relative movements (small to large in Fig. 9). For the chambers in the small sectors, alignment is done with tracks that overlap with chambers in the large sectors.
- At the third level, the global alignment system sets up a reference network that establishes a coordinate system to determine chamber locations. In the barrel, this is done with the reference grid mounted on the barrel toroid coils and a set of sensors linking neighboring layers of the small and large sectors.

For a high-precision measurement of muons, several requirements must be fulfilled by the precision chambers themselves: the initial internal geometry of the chambers has to be accurately known; deviations from the initial geometry has to be monitored throughout the lifetime of the experiment; and the locations of alignment sensors with respect to the sensitive detector elements has to be accurately known. A set of internal 3-point sensors is

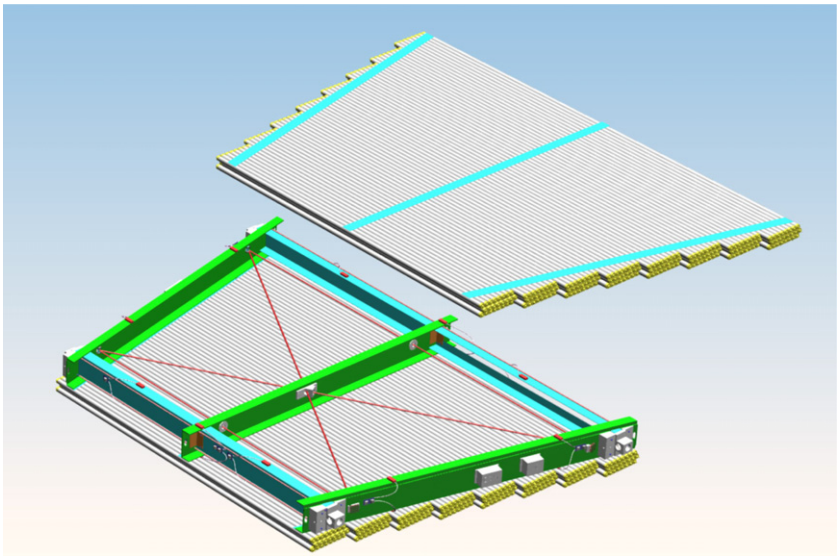

Fig. 8. An MDT chamber showing the top multi-layer of MDT tubes (gray) separated from the rest of the chamber. The spacer frame (green) contains the in-plane system. The 3-point optical lines of the system are shown as red lines. (For interpretation of the references to color in this figure legend, the reader is referred to the web version of this article.)

embedded in the chamber during construction. Deviation from the initial shape of the chambers is monitored over the lifetime of the chambers. This is called the in-plane system. The organization of these sensors is shown in Fig. 8. The in-plane system monitors the mechanical deformations of the chambers, and the thermal expansion information is provided by temperature sensors built into the chambers. The principle deformations are twist and thermal expansion. Not correcting for this adds $\sim$50 μm to the error in sagitta.

For the sensors that link the chambers to the global alignment system, the positions with respect to the MDT wires need to be accurately known. There are four alignment sensor mounts near the corners of each chamber. In addition there are four photogrammetry target stickers [8]. Great care was taken to relate the alignment sensors to the precision components of the muon chambers, so that knowing where the alignment sensors are gives precise knowledge of where the chambers are located.

The organization of the ATLAS magnets, a solenoid for the inner tracker and 3 toroids for the muon system, means the inner detector (which measures momentum in the r–ϕ projection) and the muon system (which measures momentum in the r–θ projection) are essentially orthogonal. Muon momentum can be measured as a stand-alone muon system, as a statistical combination of the inner detector and muon system, and by joint fits to the inner detector and muon system. All three approaches are in use.

The second level of the alignment system uses a reference grid to establish a unique coordinate system. In the muon barrel this is called the "reference system" [9]. This system consist of plates mounted on the barrel toroid ribs and has CCD cameras that look at targets placed on plates on the same coil and two adjacent coils, making possible a 3D reconstruction of the reference plates and hence coil positions. Cameras also look at targets placed on neighboring chambers. The chambers are then connected together with a series of optical lines using RASNIK sensors in a variety of applications. A set of optical lines for the barrel alignment system is shown in Fig. 9.

The backbone of the global alignment system for the endcap muon system (see Fig. 10) is a set of precision reference rulers, called alignment bars. These bars establish a precise grid in space, relative to which the positions of the precision chambers can be measured in a second step. The positions of alignment bars with respect to each other are determined by sensors mounted on the bars that are looking at each other. The positions of the precision chambers with respect to the bars are determined by sensors on the chambers, looking at light sources on the bars or on neighboring chambers, and vise versa.

The alignment bars [10,11], are constructed with an internal set of overlapping RASNIKs and temperature sensors (see Fig. 11). A detailed mechanical model of the behavior of the bars, plus corrections from the internal RASNIKS, allows us to follow the location of the sensor mounted on the bars over the lifetime of the alignment system, even when the bars change gravitational orientation and temperature. Studies have shown that we can follow the behavior of even the longest bar (9.6 m) with a precision of 15 μm.

Eight alignment bars are embedded in each layer (wheel) of the endcap muon system. Polar optical lines link alignment bars in different wheels. A polar line consists of a triplet of polar BCAMs, each one on a different bar, arranged approximately on a straight line, in such a way that each of the 3 BCAMs can monitor the positions of the other 2. The polar BCAM in the middle is therefore always double-ended, with cameras facing both ways. Between each pair of adjacent alignment bars within a wheel are as many azimuthal lines as there are large–small MDT chamber pairs. At least one azimuthal line between each pair of bars is not parallel to the others. An azimuthal line consists of a pair of azimuthal BCAMs, 1 on each bar, where each one monitors the position of its partner. Two azimuthal lines are sufficient to determine the positions of the 2 bars with respect to each other. Where there are more than 2 lines, they are eventually needed for the proximity measurement, but in this case just provide redundant information. By considering all 8 bars in a wheel, and eventually all 48 bars in one endcap, it becomes clear that the grid system is highly over-determined, and thus its precision deteriorates only mildly in case of single BCAM failure. The fitting process locates all the lines with respect to each other. Including some of the collision hall survey targets in the fit fixes the alignment bar grid to the accelerator coordinate system as determined by the surveyors. In this sense, it is an absolute determination of the grid location.

The connection between the 247 MDT chambers in one endcap and the reference grid is primarily established by the proximity sensors. Typically, a large and a small MDT chamber are linked to

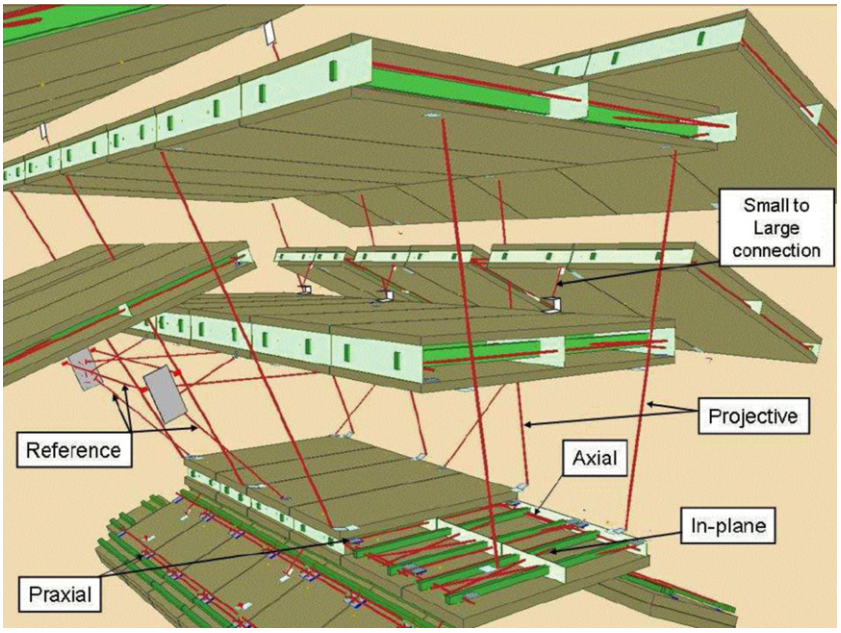

Fig. 9. ATLAS barrel alignment system showing the optical alignment connections (red line) in 3 adjacent sectors. (For interpretation of the references to color in this figure legend, the reader is referred to the web version of this article.)

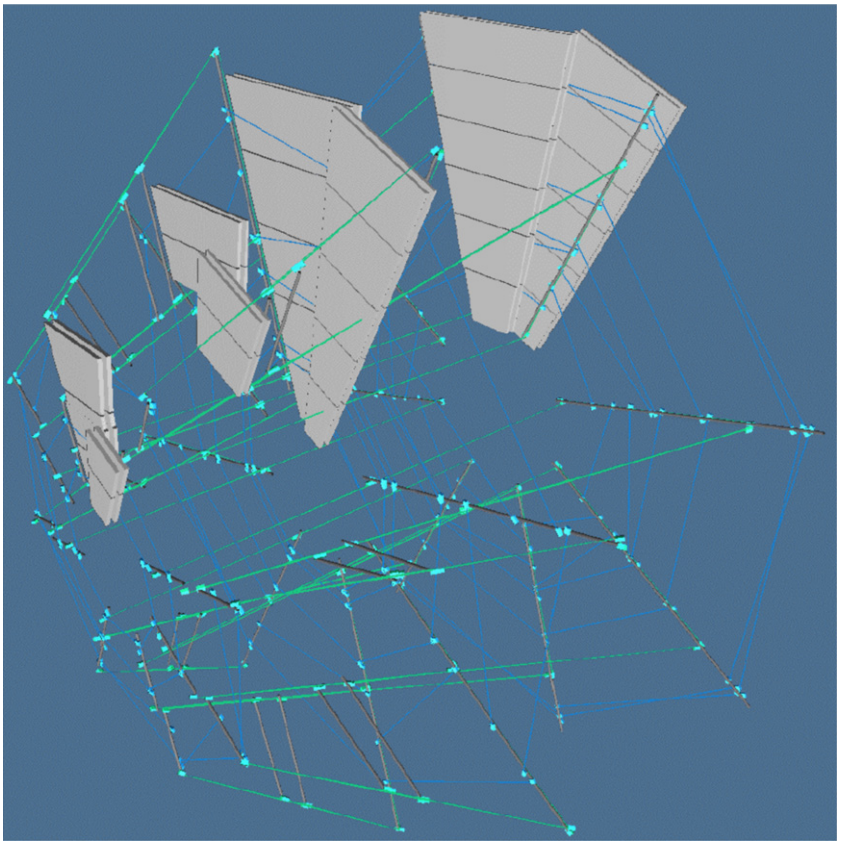

Fig. 10. Layout of alignment bars in the MDT endcap region. This figure shows the layout of the alignment grid in one endcap of the muon spectrometer. MDT chambers are shown only in one (of 8) large sector and one (of 8) small sector. The optical connections between the 48 alignment bars are shown, the azimuthal connections in blue and the projective connections in green. The projective connections point approximately to the interaction point at the center of ATLAS. All of the optical connections terminate at BCAMs. There are cutouts (not shown) in MDT chambers for optical connections that pass through chambers. (For interpretation of the references to color in this figure legend, the reader is referred to the web version of this article.)

each other and to the 2 adjacent alignment bars via a network of sensors, shown in Fig. 12. Proximity cameras on the 2 outer edges of the chambers in the pair view RASNIK masks on the alignment bars. In addition, there is one camera-mask pair where the camera is mounted on the large chamber and the mask is mounted on the small chamber. Finally, on the remaining corner of the large and small chambers, there is one chamber laser source on each chamber that is viewed by azimuthal BCAMs on the alignment

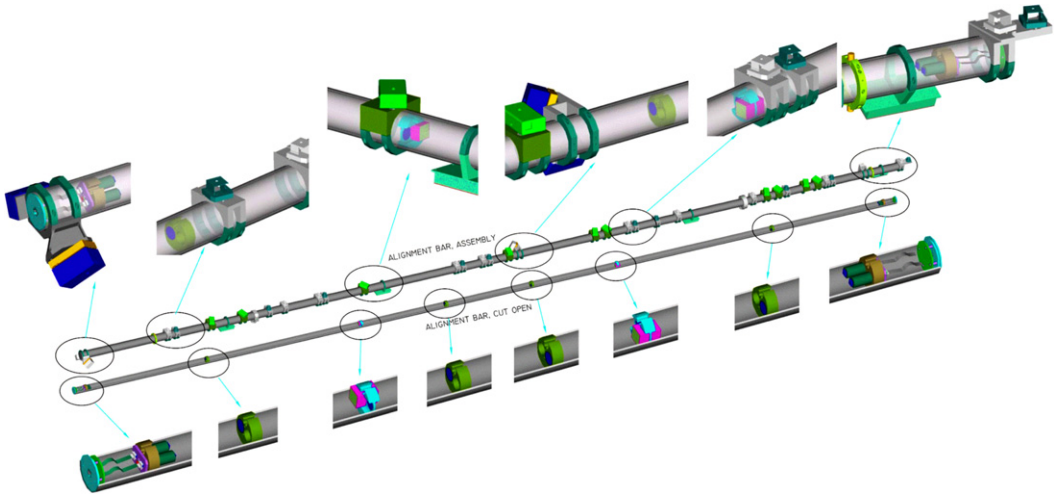

Fig. 11. A 9.6 m alignment bar for the EM layer of muon system. Clamped onto the bar tube are platforms with sensors mounted on them, as well as the kinematic mounts. Detailed views show, from bottom to top: a polar and a radial BCAM; the gimbal mount; an azimuthal BCAM; 2 proximity masks; slip-ring mount; and a ring for inserting survey targets, together with readout multiplexers and 2 proximity masks on a special platform. Attached to the inside of the tube are disks holding components of the in-bar RASNIK system. Detailed views show, from bottom to top: 2 CCDs; a lens; a lens and 2 masks; and a disk without optical elements. The remaining 4 views are the same as the first 4, in reverse order. The 8 in-bar temperature sensors are attached to these disks.

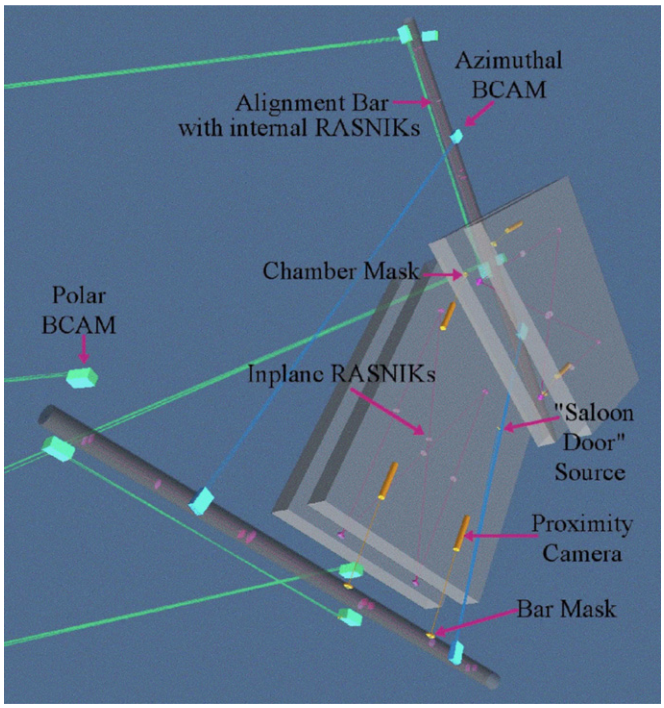

Fig. 12. Layout of the MDT proximity system in a typical pair of sectors. Shown is a large–small MDT chamber pair. Alignment bars overlap with the small chambers. The figure shows the 3 components of the proximity system: 2 proximity cameras on each chamber viewing masks on bars; 1 proximity camera on each large chamber viewing a mask on the small chamber; a pair of azimuthal BCAMs on the bars viewing one chamber laser source on each of the two chambers. The azimuthal BCAMs are, at the same time, part of the reference grid system, and the azimuthal line passes through the 10 mm gap between the 2 laser sources. All the sensors of the proximity system are located in the space between large and small chamber layers in a wheel.

bars. These sources are the reason why the number of azimuthal lines matches in each wheel at least the number of chamber pairs. This design locates both chambers in the pair to about 30 μm and 100 μrad with respect to the adjacent bars. To align the ATLAS muon system requires a large number of alignment devices. In the barrel system there are almost 6000 sensors including 2110 RASNIKs measuring chamber deformation, 3191 RASNIKs locating chamber positions and 516 SaCams linking the small and large towers and the chamber to the barrel toroid. In the endcap there are over 6000 sensors including 1984 RASNIKs measuring chamber deformation, 272 RASNIKs and BCAMs measuring bar deformations, 2384 RASNIKs and 586 BCAMs measuring MDT chamber positions relative to alignment bars, and 944 BCAMs measuring the relationship among the bars.

CMS is built around a large and powerful 4 T solenoid. The CMS magnet and muon detector are described in detail in Ref. [2]. In Ref. [3], a motivation of the main parameters is given. The choice in the muon chamber parameters (intrinsic spatial resolution, dimension, and materials), together with the stringent quality control procedure during the construction phase of the chambers, allows considering them as single rigid bodies at the level of 100 μm, therefore relaxing the requirements on active internal chamber alignment monitoring.

The muon chambers in CMS are interleaved in the return yoke (see Fig. 2). In the central part (barrel), the shape of the iron is divided in 12 trapezoidal wedges or sectors, to better simulate a cylindrical geometry. The muon chambers are located in pockets between 3 layers of iron. In the each endcap, they are attached to the surface of the 3 iron disks. An important feature of the CMS muon spectrometer is the fact that the return yoke is made out of 11 independent and large structures (5 wheels in the barrel part and 6 disks at the 2 endcap sides) that can be separated for maintenance by sliding along the beam line. The huge magnetic field of the CMS solenoid generates strong forces that compress the 5 wheels and displace and deform the endcap disks. Although the size of these displacements is significant, up to a few centimeters, the effect of the magnetic forces on the detector structures is quasi-elastic. As can be seen in Fig. 13, the same spatial coordinates are almost completely recovered after magnet cycles.

Muon momentum can be measured by the radius of curvature of the track, the bending angle, ϕ, or by the sagitta. The most precise measurement is obtained when using the full bending power of the CMS solenoid, which requires combining the information of the tracker and the first muon station. The stringent position measurement precision applies to the coordinate in the bending plane, r–ϕ. A complete simulation of the detector, including all known sources of possible systematic effects, was used to

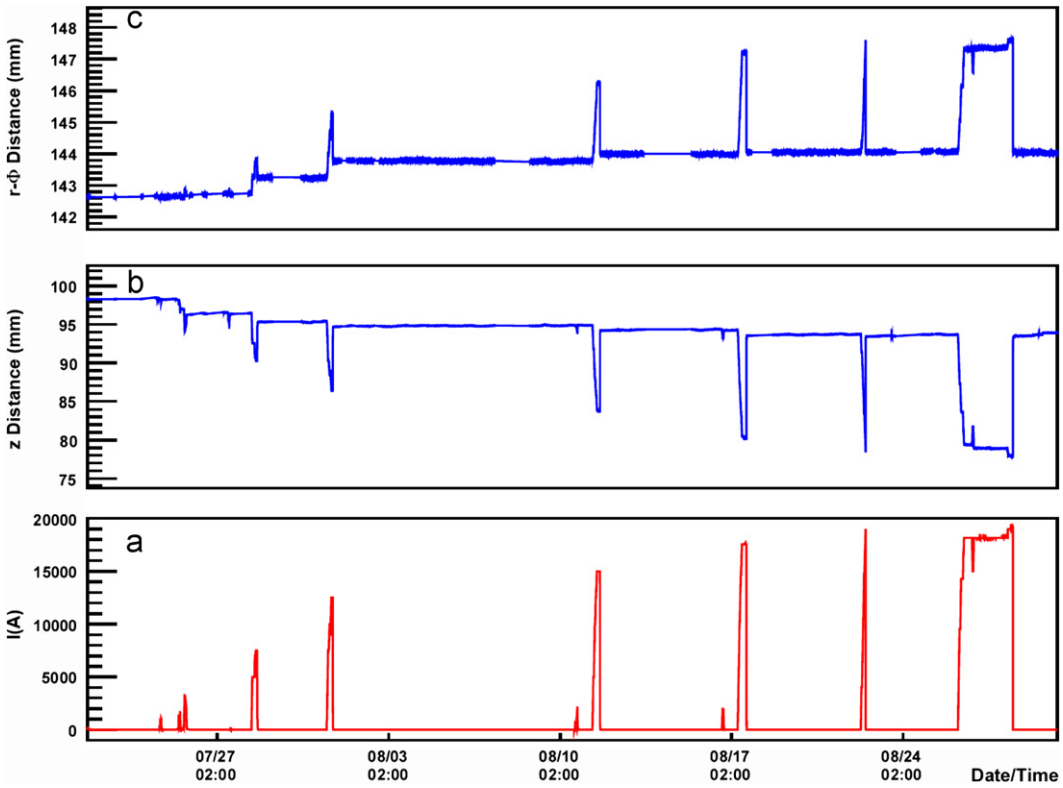

Fig. 13. Deformations of endcap disks and barrel wheels vs. magnet current cycling. The bottom plot shows the magnet powering cycle exercised during the test of the CMS magnet. The top plot shows the measured first endcap disk deformation in r–ϕ coordinate. The middle plot shows, for the same structure, the measured z coordinate vs. the magnet current, illustrating the compression toward the interaction point.

establish the alignment precision requirements for the entire muon momentum range up to 1 TeV. Muon chambers must to be aligned with respect to each other and with respect to the central tracking system to within a few hundred microns in the r–ϕ coordinate. The required precision for the endcap chambers ranges from 75 to 200 μm, depending of their distance to the interaction point. Due to the radial strip pattern of the endcap muon chambers, a precision measurement in the radial coordinate at the level of 450 μm is needed to guarantee that no error is propagated into the precise ϕ coordinate. For the barrel, the precision varies from 150 μm for the inner chambers in the first station to 350 μm for the outer chambers of the fourth station; the requirements on the other coordinates are less stringent.

In CMS, the alignment system [12,13], is organized in 4 main building blocks

- An internal alignment of the inner tracker, as discussed above, to measure positions of the different tracker detector modules and monitor internal deformations, such that it allows to consider the tracker as a rigid body, for the rest of the detector systems.
- Local alignment subsystems of Barrel and Endcap muon detectors to monitor the relative position of the muon chambers within each detector subsystem.
- A link system to relate the muon (barrel and endcap) and tracker alignment systems, and allow a simultaneous monitoring with respect to a common light-based internal reference.

The joint inner/muon alignment for CMS is needed because the muon goes through a purely solenoidal geometry so the entire track contributes to the resolution. For ATLAS the inner tracker (solenoid) and muon (toroid) are orthogonal measurements so a joint measurement is not significantly better than combining tracks.

Fig. 14 shows schematic views of the CMS alignment system. The inner tracker system has been already described, a detailed description of the muon alignment systems has been presented in Refs. [2,3].

The layout of the system was defined to preserve the hermeticity of the detector. As shown in Fig. 14, the system has a 6-fold segmentation, following the 12-fold barrel muon segmentation. The lines of sight follow the natural paths in the detector, which do not always correspond to the most direct connections among detector parts. Rigid and low mass carbon fiber structures, Link Disks (LDs), and Alignment Rings (ARs), sitting at the tracker end plates and at the first endcap iron disk, act as light-source support and help define the light-path geometry of the global reference system thanks to mini-optical bench precisely mounted on these structures. Modules for the Alignment of the Barrel (MAB) attached to the barrel yoke act as the backbones of the barrel muon alignment system and serve to relate the different alignment subsystems in the muon region.

Although not visible in Fig. 14, the alignment components do not interfere with the active detection volume of the muon chambers; therefore the acceptance of the detector is not modified. As a drawback, the price to pay is a more complicated (less precise) transfer of information from the actual measurements to the active detector units. This mechanical transfer, usually via precise pin, must be solved by means of precise chamber construction, sensor referencing, and dedicated optical and/or mechanical survey measurements.

A peculiar part of the CMS alignment, not present in the ATLAS design, is the Link System, whose main function is to link together the 3 CMS tracking detectors (the Barrel, the Endcap Muon, and the Tracker), measuring and monitoring the relative position of the central tracker with respect to the Muon system, but mainly with respect to the first station. The key elements are 2 carbon

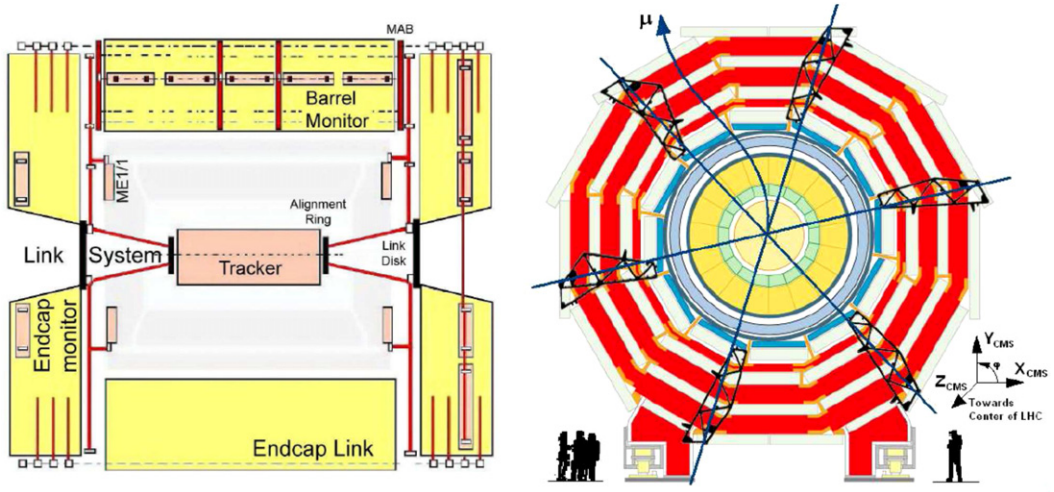

Fig. 14. Schematic view of the CMS alignment system. Left: longitudinal view of CMS showing one of the 3 *r*CMS–*z*CMS alignment planes. The continuous and dashed lines show different optical light paths. MABs on YB+1 and YB−1 are not shown because they are rotated 30° with respect to this plane. Right: transverse view of the barrel muon detector. The crossing lines indicate the *r*CMS–*z*CMS alignment planes with 60° staggering in ϕ.

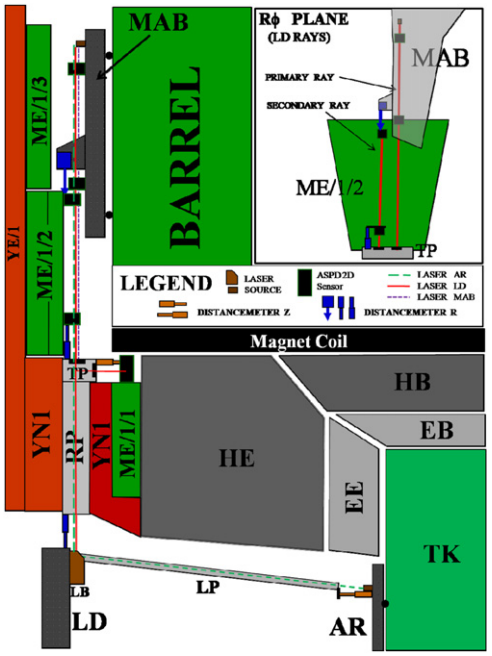

Fig. 15. Details of a quarter of a plane of the CMS Link system.

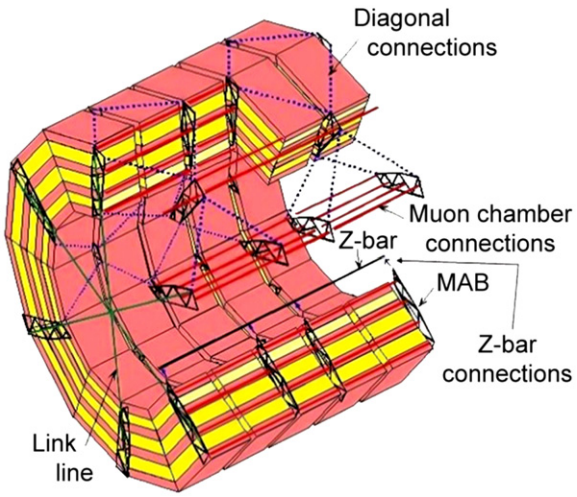

Fig. 16. Schematic view of the barrel monitoring system showing the optical network among the MAB structures.

fiber rings (LD) supported by the first endcap iron yoke at the 2 opposite sides of CMS. Their diameter is 1300 mm and they are positioned at about $\eta=3$, centered with respect to the beam line. They are supported by 3 long aluminum bars attached to 3 of the 6 reference plates (Transfer plate; see Fig. 15) attached to the iron at the outer border of the nose in the first endcap disk. Radially oriented laser lines generated at the LD (Laser Box, LB) are detected by photo-sensors placed on MABs and endcap muon chambers. Some of them are visible in Fig. 15. Distance and angular measuring devices complement the optical measurements. Two carbon fiber rings (ARs) with a diameter of 730 mm are on the outer external faces of the tracker, attached to the support plane of the outer silicon layer of the tracker endcap. They are equipped with 6 laser collimators and 3 distance sensors. The laser lines reach the LD and are deflected radially and detected in the MABs by the same sensors that look at the lines generated by the LD itself. The relative displacements of the AR planes with respect to the LD are monitored by the 3 distance sensors and by the long aluminum tubes (LP), supported by the LD. It is worth noting that hermeticity and space constraints dictate that the connection of the AR to the tracker volume is accomplished by the precise mechanical attachment of the AR to the most external tracker flange. Thus the 2 sides of the Link System, forward and backward, are weakly linked with each other, as well as to the internal tracker alignment.

The barrel and endcap muon detectors are defined as stand-alone systems [14]. In the barrel part, the muon chamber positions are monitored with respect to a network of 36 rigid mechanical reference structures, MABs, optically connected with each other and fixed to the barrel yoke, forming 12 *r*–*z* planes parallel to the beam line and distributed in ϕ. Six of them are connected to the tracker laser lines, though the MABs located on the external barrel wheels. The network layout is shown in Fig. 16. MABs are instrumented with video-cameras looking at light sources located on the muon chambers or on the MABs themselves (diagonal connections). The muon chambers are equipped with sets of 6–10 LED light sources, mounted on precise frames, at the 4 corners of the chamber, inside

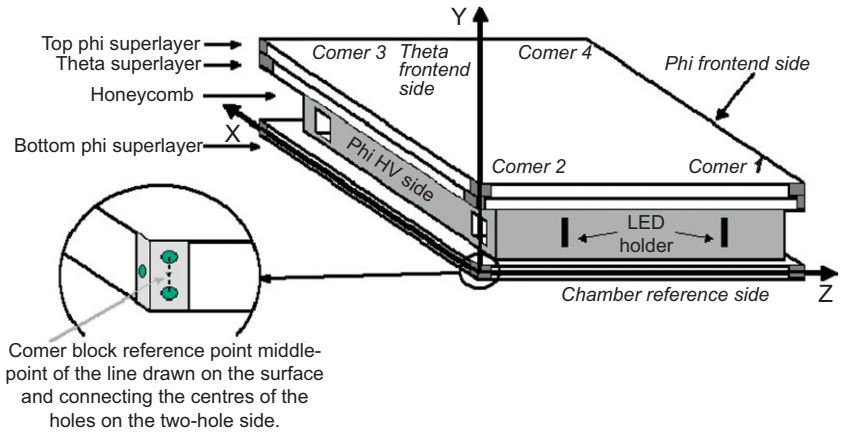

Fig. 17. Schematics of a barrel muon chamber showing the location of the light sources and the reference system used for internal calibration.

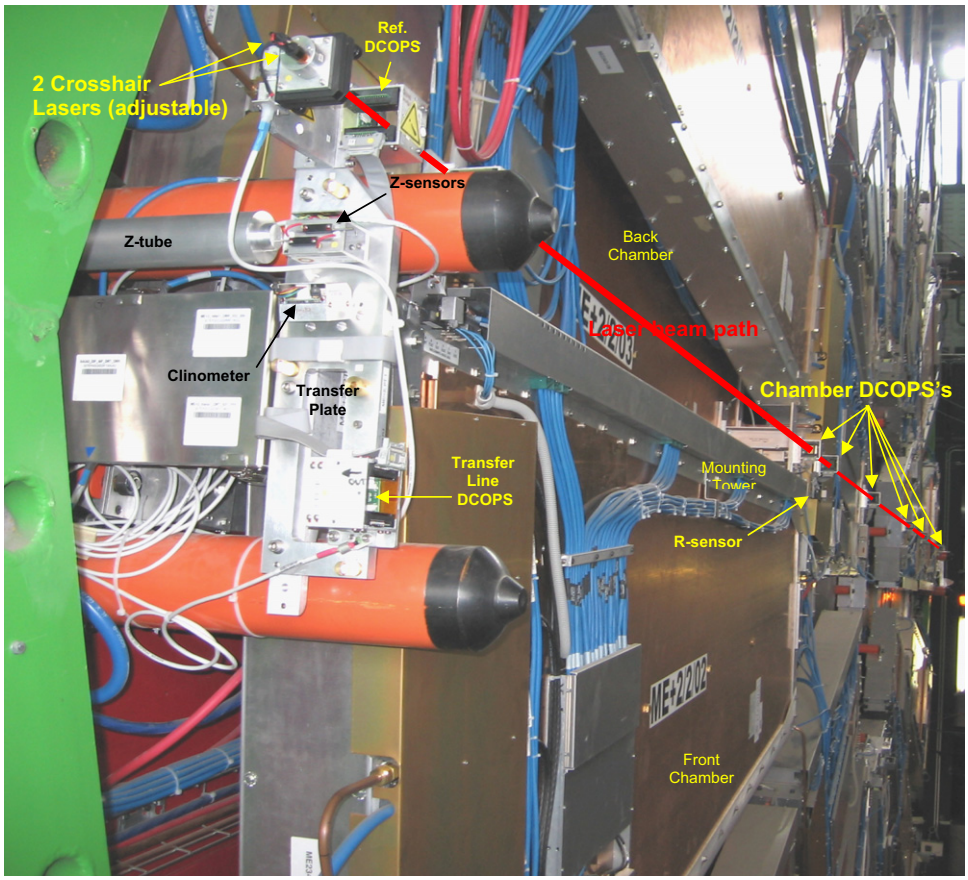

Fig. 18. Close-up of one of the 3 Straight Line Monitors (SLMs) on the second endcap station with cross-hair laser, optical sensors (DCOPS), analog sensors for r and z coordinate measurement, and Tiltmeter.

uninstrumented passages defined between the chamber superlayers. After assembly, a full calibration of the chamber geometry relates the light sources with the chamber active layers. Fig. 17 shows the schematics of a barrel muon chamber, as well as the reference system used during calibration. The system provides a strong relation between chambers in a sector as well as between adjacent sectors. The total number of independent degrees of freedom in the stand-alone barrel position monitoring system is about 3000, while the number of independent observations is more than 4000, giving the desired redundancy to the system.

Given the big deformations suffered by the endcap disks when the magnet is energized, the basic and most characteristic unit of the endcap alignment system is the straight laser-line monitor (SLM) that runs over the face of the disk, a distance of about a 14 m, measuring up to 10 position sensors in the line. An SLM is built from laser sources located at almost radially opposite locations at the outer boundaries of the endcap disks (positioned to miss the beam pipe), crossing 4 endcap muon chambers. SLM monitors provide precise r–ϕ and z information of the chambers in a given layer. Fig. 18 illustrates the complete instrumentation in one endcap layer of chambers. The system uses a complex

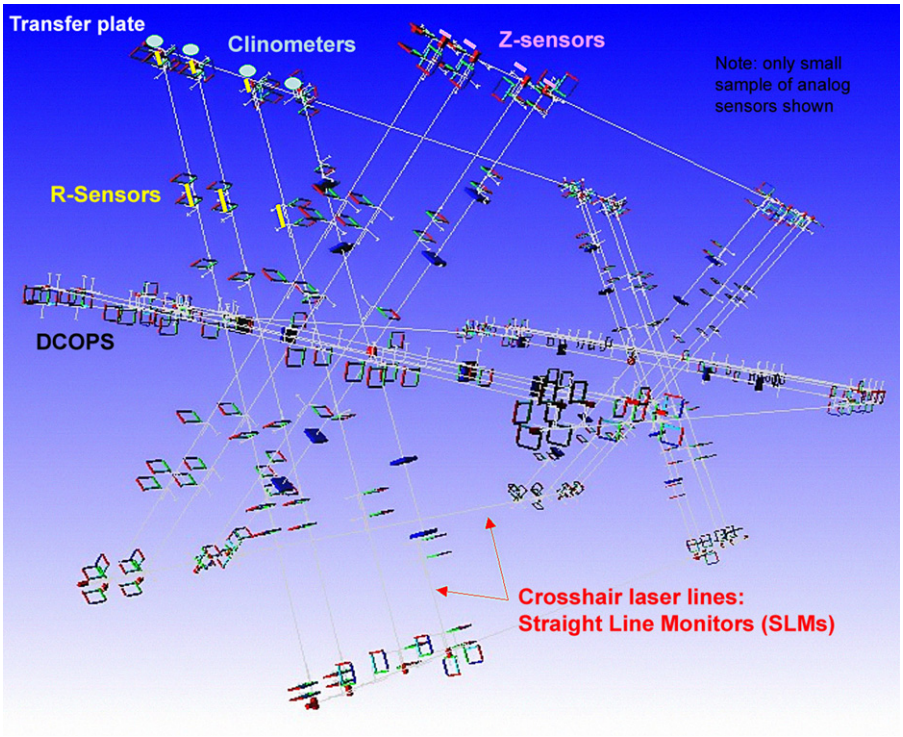

Fig. 19. Visualization of the geometry and components of the muon endcap alignment system. The square objects represent optical sensors (DCOPS) for monitoring 3 straight laser lines across each endcap station.

arrangement of 5 types of sensors for the transferring and monitoring of ϕ, r, and z coordinates. As shown in the figure, one sixth of all endcap chambers are directly monitored. The non-monitored chambers in each disk are aligned using tracks in the overlap region.

A total of 48 SLMs cover the entire endcap spectrometer (Fig. 19). The first layer of endcap chambers, most relevant for momentum measurement, is as well directly seen by the laser-lines linking the muon system with the tracker volume. Six axial lines at the outer boundary of the muon spectrometer, also shown in Fig. 19, provide an extra closure of the alignment system.

The CMS muon optical network uses 2 types of light sources: LEDs and laser beams. It is composed of 10,000 LEDs and 150 laser beams together with precise measuring devices: ~900 photo-detectors and ~600 analog sensors (distance sensors and inclinometers), complemented by temperature, humidity and Hall probes.

A general purpose software [15] developed for simulation and reconstruction of the complete alignment system was used intensively during the design phase as well as for the calibration and characterization in the laboratory of the alignment components and partial system setups.

2.3. Further remarks

Despite the different geometries of the ATLAS and CMS muon spectrometers, the final conceptual and implementation choices of the optical alignment systems are quite similar. Among the similarities are the factorization of the measurements, the use of internal reference networks, the practical choice of components and approach to analysis.

Although detector capabilities and precision are driven by the design on the detector, the choice of measurement technology, and the physics goals of the experiment, there are basic concepts of alignment, which transcend these particulars. These concepts include the precision of the individual alignment devices, the built-in redundancy or over-determination in the alignment system design, and the capability to factorize the reconstruction of the full detector geometry.

The precision and reliability of the system depend on the choice of its basic components. Given the large number of components, the measurement uncertainty of the individual elements should be as small as possible so that it does not have much effect on the global uncertainty budget. The system components must be simple, robust, and reliable so that they allow a direct interpretation of the measured quantity. The systems should be arranged, to the extent possible, so they measure the motions that directly affect the momentum measurement rather than try to untangle this motion from indirect measurement.

Over-determination in measurements allows the graceful degradation of the system components and helps detecting faulty measurements. It also permits cross checks between measurements, enhancing the capability to disentangle complex motions, and improves the overall resolution of the system. Yet, although desirable, redundancy is not always achievable, given the constraints and limited natural lines of sights present in the complex LHC detectors.

Geometric reconstruction by global χ^2 minimization is a process whose complexity grows as N cubed for N fitted parameters. Consequently, CPU performance could become an issue for large alignment systems, such as those implemented in LHC detectors. One efficient approach to this problem is to make use of factorization, i.e. the feature of a given alignment system design so that the alignment can be reconstructed by splitting the problem into subsets of objects to be aligned sequentially without noticeable loss of accuracy or consistency.

Although factorization is nontrivial, both ATLAS and CMS are using this property in their reconstruction sequence. As an example, the alignment of the two ATLAS muon endcaps, comprising about 10,000 fitted parameters, can be reconstructed by performing 864 small fits of 9 or 12 parameters each (bar/chamber shapes and locations of MDT chamber pairs with respect to bars, respectively), and two large fits of 384 parameters each (locations of bars and CSC chambers with respect to each other).

3. Optical alignment tools

In this section, we review the various devices used in the alignment of particle detectors. Given the specific requirements, imposed mainly by precision and space constraints, ad-hoc devices are developed and/or adapted by the various collaborating institutes involved in the design and construction of these systems. The environmental operating conditions of LHC experiments impose stringent constraints, as do the specifications in terms of radiation hard materials and magnetic field insensitivity. As mentioned in the previous chapter, the choice of reliable and robust components is one of the guidelines in the design and construction of alignment devices.

Commercially available sensors fulfilling the specifications of LHC detectors are also used as complementary devices to the laser-based systems. In particular, contact and noncontact displacement sensors and electrolytic tilt-sensors have been used for distance and angular measurements in the CMS alignment system [16]. Standard temperature, humidity and Hall probes are also used; they allow compensating environmental operating conditions.

Custom devices developed for active monitoring of particle detectors can be widely classified as

- Straight line monitors as either CCD based systems or multi-point alignment sensors,
- Absolute distance monitors, and
- Alignment structures.

3.1. CCD based systems

The principle of the system is illustrated in Fig. 20. An optical sensor looks through a lens towards a target (light source). The sensor image is analyzed and treated to find the effective source location. The output is converted in 4 parameters

- Translation of x with respect to the optical axis z.
- Translation of y with respect to the optical axis z.
- Rotation of angle $q(z)$ between the target and the optical sensor.

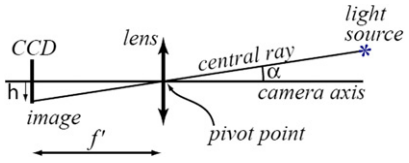

Fig. 20. Working principle of a CCD based straight monitor system.

- Magnification of the optical system (coordinate along the optical axis).

Several implementations exist, which are used as straightness and distance measurement devices. The precursor of this type of devices is the RASNIK device developed at the NIKHEF Laboratory. RASNIKS are 3-point straight line monitors consisting of a target (source), a lens, and a CCD or CMOS video-sensor. Different versions of this device have been used for monitor tracking and muon detectors in different experiments over the last decades [17]. Variation of the internal parameters can be tailored for different dynamic range applications. Usually the disposition of the 3 elements is done in a symmetric way. The latest incarnation of RASNIK devices, developed for the ATLAS experiment, is sketched in Fig. 21.

As described in Section 2 and illustrated in Fig. 8 this device has been deployed extensively in the ATLAS alignment system, where it is used mainly to monitor the stability of the muon chambers, allowing a continuous monitoring of chamber deformations and providing real time corrections.

A variation of this device, with the lens rigidly fixed to the CCD (asymmetric RASNIK), is used as distance proximity sensor. For this application, the distance lens-CCD can be tailored to cover the desired range of distance, typically between 0.25 and 0.85 m. The transverse dynamic range can be up to ± 15 mm (given by the size of the mask). Typical resolutions are: 120 μm for longitudinal displacements and about 20 μm and 50 μrad for transverse and angular displacements.

Other implementations for LHC detector monitoring, using point-like light sources, are the Brandeis CCD Angle Monitor (BCAM) [12], Saclay Camera (Sa-Cam) [11], or MAB video-cameras [Ref. 14]. As an example the BCAM device is described here.

A BCAM (Figs. 22 and 23) consists of one (single-ended) or two (double-ended) cameras, combined with 2 or 4 light sources into one solid camera body. The body is an anodized aluminum chassis, made out of a single piece of aluminum for stability and ease of assembly. In operation, the camera in one BCAM looks at light sources on another BCAM, and the camera in the other BCAM looks back at the light sources in the first camera. A BCAM camera consists of a lens and a CCD image sensor separated by 76 mm. The BCAM light sources are pairs of laser diodes with a transverse separation of 16 mm. The laser diodes are near-ideal point sources, in that their emitting surface is only tens of microns across. With an uncollimated output power of a few milliwatts, they are not harmful to the human eye, but they are visible, which makes diagnosis of BCAM problems far easier than with infrared light. The center of the light spot on the CCD can be determined to about 0.4 μm on the CCD. To improve the resolution, the lens

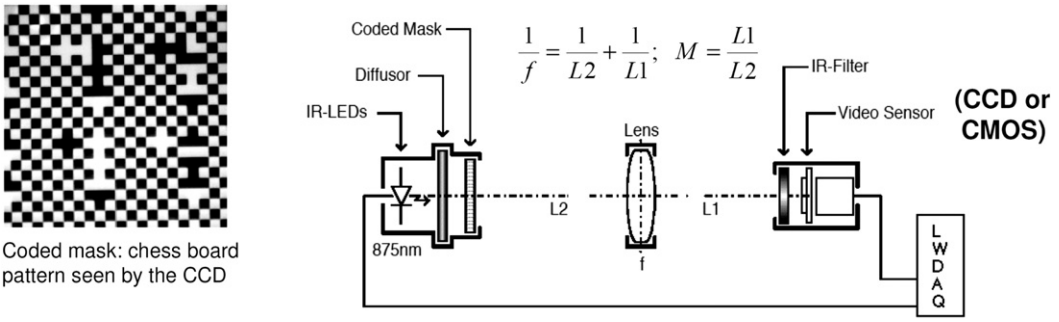

Fig. 21. Schematics of the working principle of RASNIK devices. The target consist of a mask formed by a chromium film glass slide (<0.5 mm), with a chessboard-like pattern back-illuminated by an array of infrared LEDs. A diffuser is placed between the LEDs and the film, thus smoothing imperfections due to the light source shape. The chessboard dimension D (~ 150 μm) is chosen so that the image of each square is covered by at least 5–10 pixels. This allows an interpolation of the black and white transition, thus improving the translation resolution. D varies depending on the magnification of the system. The mask size (typically 25×25 mm^2) varies depending on the dynamic range desired. Typical measured resolutions are 1 μm in the coordinates transverse to the image and 0.00005 in the magnification, M.

aperture has been chosen so that the spot is slightly blurred by diffraction, and so that the image of the laser spreads over several pixels: typically around 10–15 pixels are above threshold. BCAMs are mounted kinematically on alignment bars. The BCAMs are kinematically mounted on 3 small balls (1–2–3 kinmatic mount) that form the reference coordinate system. The BCAM is calibrated by mounting it in a "roll-cage", which can be put in 4 known orientations to view a common set of laser sources, also in known positions. From these measurements the calibration constants for the BCAMs are determined.

The calibration [18] of a BCAM is best understood if one views the camera as a point in space, called the pivot point, through which all rays of light hitting the CCD pass. This point is near, but not exactly at, the center of the lens. Any particular ray hitting the CCD corresponds to a vector at the pivot point aimed toward the source of that ray. In the coordinate system defined by the BCAM mount, the calibration constants for a BCAM are the X, Y, and Z coordinates of the pivot point, the distance from the pivot point to the CCD, the direction cosines of the optical axis (the line connecting the center of the CCD to the pivot point), and the rotation of the CCD about that axis. From this information one can compute the location of the spot on the CCD from any source of light.

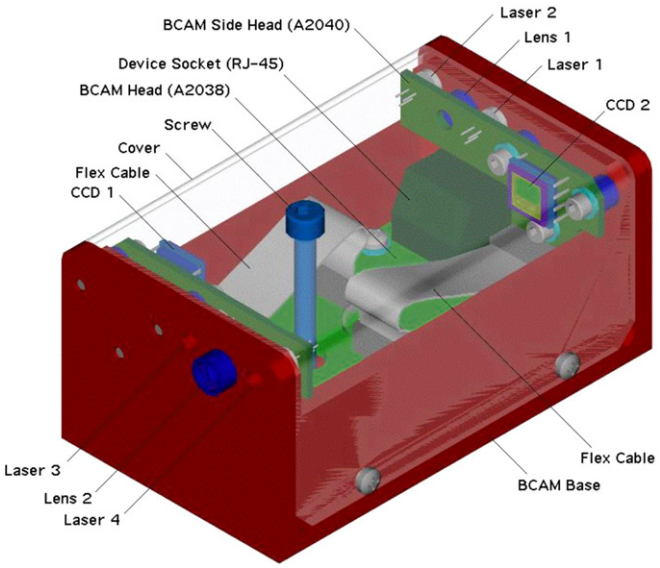

Fig. 22. A double-ended BCAM with the cover removed. On the left, the lens holder and lens of one camera are visible, with 2 laser diodes in holes next to them. The CCD of that camera is on the right. Another camera and another pair of laser diodes face the opposite direction. The electronic boards for CCDs and lasers are mounted at the bottom and the front and back walls of the chassis, connected through white flat cables. Below the lens holder is a socket to connect the CAT-5 cable for the readout system.

In a pair of BCAMs, one BCAM measures the absolute angle of the 2 laser diodes on the other BCAM with respect to its own optical axis with an absolute accuracy of 50 μrad. It also measures the difference in angles, i.e. the relative angle of those two laser diodes, with a (much better) relative accuracy of 2 μm/d, where d is the distance to the lasers. The intrinsic resolution of each individual spot measurement is 5 μrad. In a triplet of BCAMs positioned approximately, but not exactly, on a straight line, an additional measurement can be made by each of the two outer BCAMs, by measuring the relative angle of two laser diodes, one on each of the two other BCAMs, with the same relative accuracy and intrinsic resolution as above. This makes the triplet of BCAMs sensitive to deviations from straightness. In practice, the locations of the BCAMs are determined by minimizing the distance between the predicted and measured images of distant light sources on all of the CCDs. A network of BCAMs is over-determined and therefore self-locating.

3.2. Multipoint transparent optical position sensors

Several varieties of devices, all exploiting the concept of multiple measurements along a line, have been developed in the context of LHC detectors. The measurement concept is based on the use of a visible or infrared laser source that defines a straight reference line. The light passes through the detectors and the spot position in the sensors determines the deviation from straightness. The sensors are placed at the desired measurement points. Most of the devices exploit the fact that silicon is transparent in the infrared spectrum. In these cases the main emphasis in the construction of the devices is obtaining good transmittance and avoiding deflection of the beam direction when crossing the sensors. Three types of devices are amorphous silicon based sensors (ALMYs [19] and ASPDs [20]), CCD based sensors (DCOPS [21]) and crystalline silicon based sensors (for silicon tracker devices) specially treated for light detection.

The use of the active detector devices for alignment purpose has obvious advantages. This concept was originally developed and implemented in the alignment of the tracking detector of AMS experiment [22]; further development of this idea is the

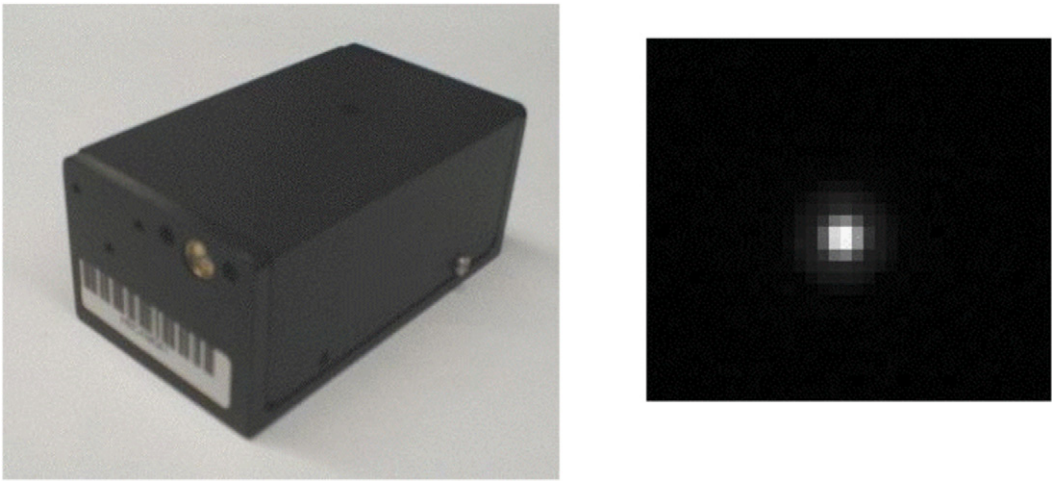

Fig. 23. An actual BCAM and an (enlarged) image as seen by the CCD. Note that the image is slightly out of focus so that it covers several pixels of the CCD; this improves the position resolution.

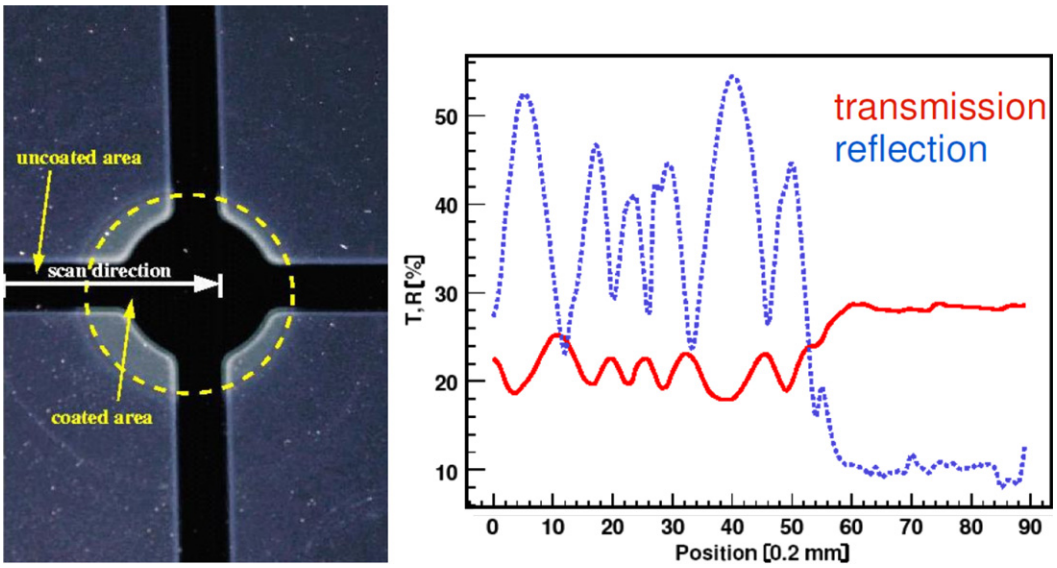

Fig. 24. Silicon sensor backplane showing the scan direction (left). Measured transmittance and reflection versus the position in the sensor (right).

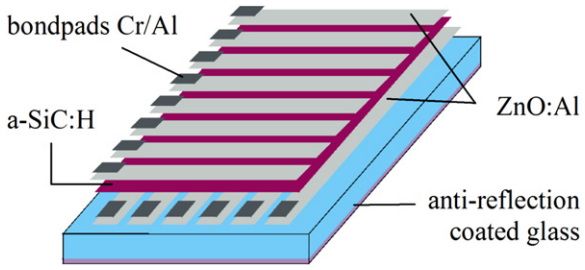

Fig. 25. Sketch of the ASPD sensor structure. The 64×64 sensor array covers an area of 30×30 mm^2 including the bond pads.

basis of the alignment of the inner tracking detector of CMS. To be used for alignment purposes, the standard crystalline silicon sensors used in the CMS tracker detector [23,24] need to follow a special treatment in order to increase transmittance and reduce multiple reflections and distortions of the beam profile. A subset of CMS silicon sensors was polished on both sides and the backplane metallization was removed in an area about 10 mm^2. The sensors were also treated with antireflective coating on the backside. To avoid undesired effects on inter-strip capacitances, no antireflective treatment was done in the strips side of the sensor. Fig. 24 shows the effect of the coating in the performance of the treated sensors in terms of transmission and deflection, using a probe laser beam with wavelength 1083 nm.

To obtain optimal signals on all sensors in a line, a sequence of laser pulses with increasing intensities, optimized for each position, is generated. A resolution better than 10 μm is obtained by averaging several measurements per intensity.

A technique based on amorphous silicon as an active material was proposed for the alignment of ATLAS and CMS muon spectrometers, and finally was implemented in CMS alignment, which required the development of 2D Amorphous Silicon Position Detecting sensors (ASPDs). The active material of these sensors is hydrogenated amorphous silicon carbide, with a 10% carbon content (a-$Si_{0.9}C_{0.1}$:H). The alloy with carbon shifts the optical bandgap of the a-SiC:H toward slightly higher values, thereby enhancing the optical transmission of the complete ASPD layer stack.

ASPD sensors are semitransparent, 2-dimensional, 28×28 mm^2 active area, strip sensors. They are deposited on top of an antireflection coated glass substrate. Special 100 mm glass wafers with a high stability against irradiation damage must be selected from a production lot for minimum deviation in parallelism of their 2 surfaces. A 195 nm layer of a-SiC:H absorber is deposited between 2 layers,100 nm thick, of perpendicular strip electrodes, made of Al-doped ZnO. An arrangement of two 1D perpendicular 64 ZnO strips enables the precise reconstruction of the position of the laser beam, while the a-SiC:H layer sandwiched between the ZnO strips provides high optical transmission and photosensitivity at the same time. The width of each ZnO:Al strip amounts to 408 μm, with a 22 μm spacing to the neighboring strips. Fig. 25 shows the layout of the sensor. Careful optimization, homogeneity, and control of all layer thicknesses ensure very high transparency for the desired wavelength of the positioning laser, by adjusting a transmission maximum of the interference fringes, to match the wavelength of the probe laser.

Each intersection of a top and a bottom ZnO strip defines a double-Schottky photodiode pixel, formed by the photoconducting a-SiC:H sandwiched between the ZnO contacts. The position of a light spot onto the sensor surface is then reconstructed as the center of the local photoresponses generated by the 2D matrix of photodiode pixels.

The final sensor implementation, adapted to the CMS muon alignment needs, is shown in Fig. 26.

The measured performance [25], in terms of average values over the full production sample

- a high sensor photosensitivity of 16.3 ± 7.6 mA/W,
- spatial point reconstruction resolutions of the light spot position on the sensor active area of $\sigma_x = 5.2 \pm 2.6$ μm and $\sigma_y = 5.1 \pm 2.4$ μm,
- very small beam deflection angles, $\Theta_x = -1.1 \pm 2.8$ μrad and $\Theta_y = 0.8 \pm 2.6$ μrad, and
- a high transmission power, $T = 84.8 \pm 2.9\%$.

An effort has been made to insure single-mode operation and Gaussian profile propagation of the laser beam.

The third type of multipoint sensors is a fully transparent version, based on a set of four CCD linear sensors arranged in window geometry the Digital CCD Optical Position Sensors (DCOPSs), The total transparency refers only to the laser beam direction, which is not affected by refraction, dispersion, or attenuation from the preceding sensors. However, a DCOPS may partially block the light going to the sensor behind it. The working principle is sketched in Fig. 27.

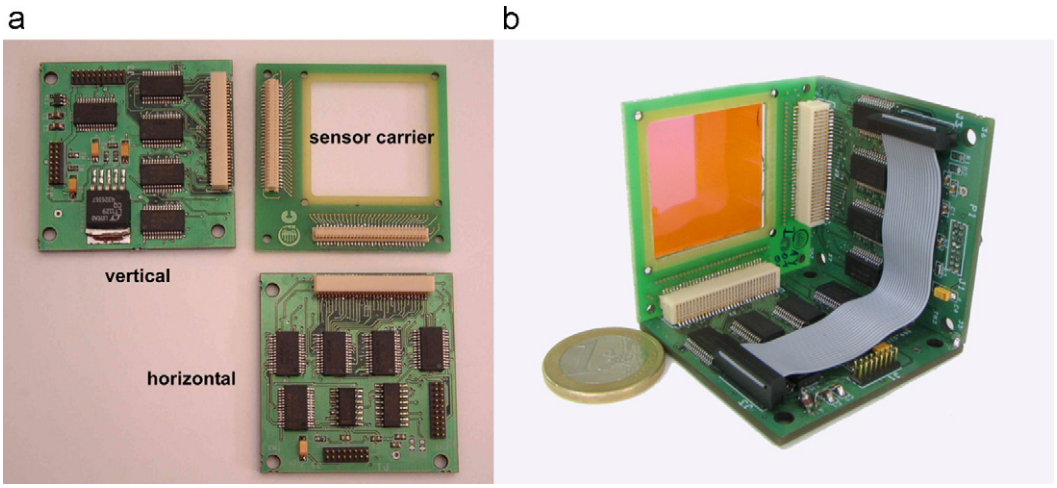

Fig. 26. Photograph (a) shows the sensor carrier board with place for sensor accommodation and 2 perpendicular lines of 64 aluminum terminated pads for sensor electronics bonding. The horizontal and vertical boards of the ASPD FE electronics, show the various components: resistors, capacitors, the 16:1 multiplexers and the "male" miniature connectors to extract the signals. Photograph (b) shows the final compact form for the 3 dimensional solution cited in the text. Dimensions are: $4.7 \times 4.7 \times 4.7$ cm^3.

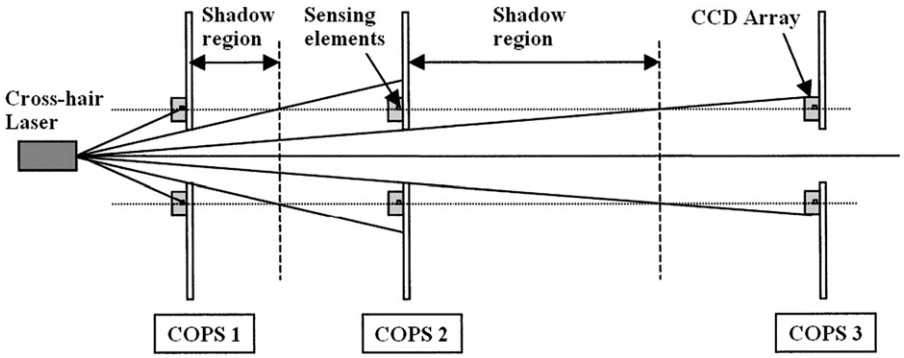

Fig. 27. Schematics of a DCOPS configuration. The first DCOPS must be far enough from the laser source to allow the beam to diverge and illuminate the CCD sensors. Subsequent DCOPS should be separated enough to avoid the shadow from the upstream DCOPS.

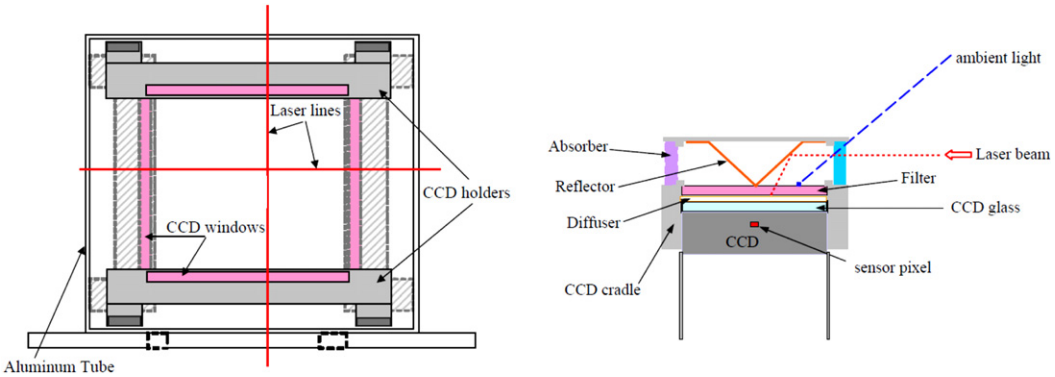

Fig. 28. Front view schematics of the DCOPS, showing the intersection with the cross-hair laser beam. The CCDs inside the holders will detect the small segment of the laser line going through the CCD window, and will measure its position (left). Schematics of CCD holder and CCD, showing the components necessary for a bidirectional CCD sensor (right).

CCD sensors have good sensitivity to visible laser light, excellent granularity (small pixel sizes), low cost, and they are readily available; they are therefore well suited for use as position detectors. CCDs come in two types: linear and surface CCD. Linear CCDs have the advantage of covering a larger range of motion (about 25 mm in CMS). When a laser line hits a linear CCD, each pixel element acquires a charge proportional to the intensity of the illumination. The charge distribution, along the array, can look like a Gaussian curve, and the centroid of that distribution defines the position of the laser line it covers a total of 28.67 mm. The position resolution of the laser line gets degraded near the ends because the beam profile is partially cut off.

The DCOPS (see Fig. 28) is a bidirectional device; it can be used with the laser beam coming from the front as well as from the back and is made out of: a box enclosure, 4 CCD cradles, and 4 front end electronics boards. The box enclosure is cut from a

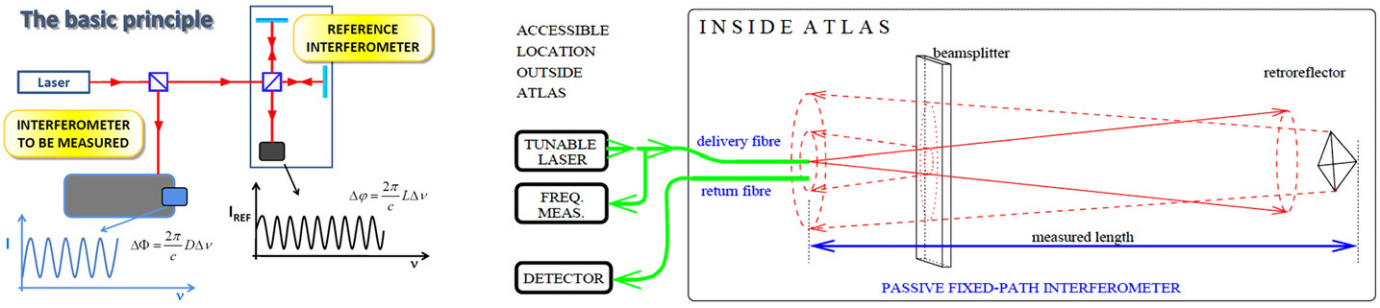

Fig. 29. Basic concept of the FSI system (right). FSI components inside and outside ATLAS detector (left).

70 mm^2 aluminum tube. Screw holes are drilled on all 4 sides to attach the 4 CCD cradles. The dimensions of the box can be varied, but the minimum inside clearance should be larger than the CCD length (42 mm). The CCD holder (Fig. 28, right) is a small black plastic frame, slightly larger than the CCD chip and containing the reflector (used to reflect the laser line coming from either of the 2 opposite directions into the CCD window), filter, diffuser, and absorbers (used to regulate the light intensity at the different distance sensors-source).

As displayed in Fig. 27, the light source is a cross-hair laser beam. The simplest way to obtain a cross-hair beam is to use two separate diode-laser line-generator assemblies, with the cylindrical lenses orthogonal to each other. A more compact solution is to use a single diode-laser whose beam goes through the 45° splice between 2 cylindrical lenses, attached side by side with perpendicular axes.

Calibration for optical DCOPS's consist of determining the distance from the surface of the mount hole for a reference dowel pin to the first active CCD pixel and measuring the projected pixel pitch of each of the 4 CCDs. A simple geometry reconstruction based on coordinate-measuring-machine data for the calibration mask and sensor mounts determined the physical pixel positions. For a given mounting, calibrations repeatability is very good (within a pixel) and the typical uncertainty in the centroid position from a Gaussian plus quadratic fit to the beam profile shape is ~3 μm. The dominant calibration error is due to the fit tolerance of dowels, this gives a typical error of 30–50 μm [26].

3.3. Interferometric distance measurement

High-precision distance measurements can be performed using the concept of Frequency Scanning Interferometry (FSI) [27,28]. The basic principle is illustrated in Fig. 29. A narrow line-width tunable laser simultaneously illuminates multiple interferometers to be measured and a reference interferometer. The optical frequency is scanned and a phase shift is induced in all interferometers at a rate that is proportional to the length of each instrument. The phase shifts in the interferometers are compared to determine the ratio of path lengths.

The technique based on FSI provides precise, O (1 μm), 1D absolute distance measurements, over distances of ~1 m. For its application to large detector volumes, a survey system is built based on large number of simultaneous 1D interferometer measurement of absolute distances between selected points in the detector (see Fig. 30). One such system has been implemented in the inner tracker detector of the ATLAS experiment. Following the strict requirements imposed by the operating conditions characteristic of LHC experiments, the implementation is based on the use of robust and maintenance-free components inside the detector. In particular, the interferometers should be small, made from radiation hard materials and have low mass. Fig. 29 (right) shows a sketch of the components inside and outside the detector. The solution is a fiber coupled interferometer [29] for each line of the grid, the main component consisting of 2 parallel single-mode fibers and a fused silica beam-splitter. The other end is a retro-reflector.

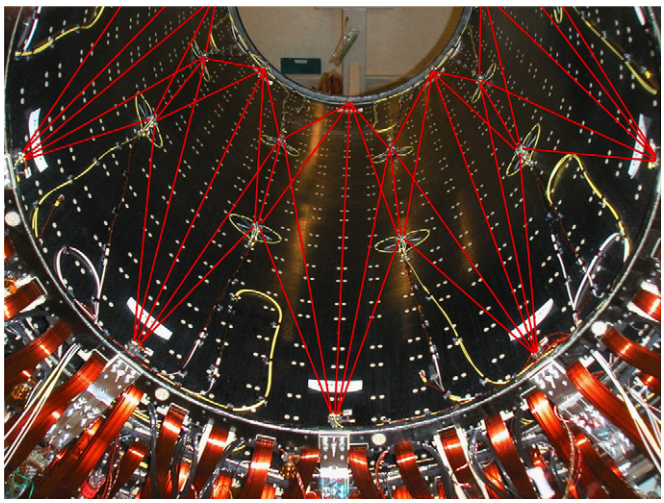

Fig. 30. ATLAS SCT barrel "on detector" FSI geodetic grid. 80 grid line interferometers are formed between 32 FSI nodes.

3.4. Alignment support structures

Both ATLAS and CMS muon alignment systems make use of a large number of support structures whose main functionality is to create an internal reference grid network. Grid layout is strictly dependent on the geometry of the monitored elements. These structures are the backbone of the global alignment systems, providing a set of precision reference rulers. They are characterized by a precise internal geometry, obtained by construction and calibration. They are built from rigid, and low mass carbon fiber material or monitored aluminum structures. Examples of such structures are the set of alignment bars used in the muon endcap ATLAS alignment system, or the MABs and Alignment Rings, carbon fiber structures used by the CMS muon alignment.

ATLAS alignment bars establish a precise grid in space, relative to which the positions of the precision chambers can be measured in a second step. The positions of alignment bars with respect to one another are determined by sensors mounted on the bars, facing each other. The positions of the precision chambers with respect to the bars are determined by sensors on the chambers looking at light sources on the bars or on neighboring chambers, and vise versa. In CMS, MAB structures follow similar logic. The positions of MABs with respect to each other are determined by sets of LED sources and sensors mounted on the MABs, facing each other, while the position of the precision chambers with

Fig. 31. CMS alignment stand instrumented with a precise survey network for the calibration of the instrumented alignment structures: MABs and Alignment Rings. The black structure in the center of the picture is a MAB in its calibration position.

respect to the MABs is determined by sensors on the MABs aimed at light sources located on the muon chambers.

These two types of structures differ by shape and dimensions, in each case adapted to the monitored geometry, but mainly, they differ regarding the choice of material. CMS MABs are carbon fiber structures. The tube shape and material are optimized to minimize humidity and temperature effects. Given the length of ATLAS bars, the chosen material is aluminum. The actual bar geometry is obtained by active monitoring of the structure, as described in Section 2.

CMS carbon fiber structures, MABs and Alignment Rings are instrumented with precise insert and alignment pins to facilitate precise positioning, and repositioning, of the alignment components housed in the structure. A large side alignment stand (Fig. 31), instrumented with a precise and stable survey network, allowed the calibration and characterization of the instrumented structures prior their installation in the detector.

4. Geometry reconstruction and initial performances

The simulation and geometrical reconstruction of the data provided by the optical alignment system are handled by programs used to study optical systems through a geometrical approximation based on nonlinear, least squared fit. These programs are in principle suitable for any alignment problem, and not specific to a given detector geometry.

The main feature of these software programs is their precise description of the optical elements within the detector, taking into account all the individual sensor calibration constants that have previously been measured in sensor calibration. Each program then converts the current sensor measurements into chamber positions using standard fitting methods. The resulting data are stored in a table in a database for later use by the muon tracking software programs.

The basic idea of this software is to construct the representation or model of the system through the description of the different system elements, their interconnections and hierarchical dependencies. The derivatives of the positions and angles of the system elements with respect to measurement values are obtained by a numerical method. The program uses the set of known components given in the system description, and composes an idealized system, from which it generates a set of ideal measurements that can be compared against the actual measured set. Based on these comparisons, it reconstructs the system geometry, taking into account the errors provided, by making variations in the positions and orientations of the modeled components. The output from those programs is the set of parameters that best fits the data and supplies the optimal solutions, so that the ideal measurements modeled by the program come as close as possible to the real measurements.

The software allows the reconstruction of the position and orientation of the optical system objects, and performs the error propagation calculation. It makes useful information accessible, e.g. about convergence and quality of the fit, and the errors and correlation matrices of all the fitted parameters.

Although the mathematical approach is common, ATLAS and CMS have developed independent simulation and reconstruction programs for their specific applications. CMS uses an object oriented C++ software (COCOA) [17] able to fit a very large number of parameters in a fraction of the time required by conventional methods. For the CMS muon alignment system, COCOA works with $\sim$30,000 degrees of freedom. The number of parameters together with the number of degrees of freedom measured by the system gives the level of redundancy with which the system is built. The complete software chain was validated [30] following the fitting-steps strategy as applied for data reconstruction.

In the ATLAS muon system, the alignment of the barrel and endcap is performed separately. Image parameters from sensors are collected periodically (from one to every few hours). From these data the MDT positions and deformations are determined by the alignment programs, Alignment Reconstruction and Simulation for the ATLAS Myon Spectrometer (ARAMyS) for the endcap and ATLAS Spectrometer Alignment Program (ASAP) for the barrel. In ARAMyS a bar shape function and a chamber shape function were implemented to take into account deformations and expansions of alignment bars and MDT chambers, respectively. The ARAMyS program consists of about 3000 lines of code written in C. For the χ^2 minimization in the alignment fit, the standard package MINUIT [31] is used. MINUIT has been used and tested for decades, and is a mature and reliable piece of software.

For debugging purposes, ARAMyS provides additional information, such as the χ^2/ndf of the alignment fit, and the contributions of individual sensors to χ^2. For this application, the sensor readout values from an actual setup are replaced by the expected measurements, which are randomly distributed by an amount that reflects the intrinsic resolution and the accuracy of the mounts of individual sensor. The alignment is then reconstructed by using these simulated measurements. A figure of merit is computed from the difference between true and reconstructed chamber positions. An accurate prediction of performance is an invaluable aid in the design process.

These programs were used extensively in the design phase of the experiments, to simulate the performance of the alignment system designs based on the foreseen network of sensors and their expected resolutions. Similarly, during the construction phase, they were used to analyze the data from the calibration campaigns of components or representative parts of the systems. For example, before ATLAS was built, a full-scale mock-up of one sector of both the barrel and endcap chambers was setup in the H8 beam line at CERN. Over a period of 3 years, the alignment hardware and data acquisition programs were developed and tested. Work in the test beam validated the design and provided a platform for extensive system testing. In addition to normal variation in chamber location, chambers were moved in a controlled fashion to validate the resolution and dynamic range of the sensor and alignment system as a whole. The overall resolution for the endcap muon chambers was estimated to be 40 μm on track sagitta.

4.1. Commissioning and validation of the reconstructed geometry

Alignment results on the reconstructed geometry must be validated before they can be used for track reconstruction. Until a precise track-based independent alignment is available [32] for the CMS muon spectrometers, the accuracy of the measurements provided by the optical alignment system is estimated by comparing the reconstructed geometry before the magnet is energized with photogrammetry measurements performed after the closing of the detector. Survey and photogrammetry of the muon chambers and detector structure are performed during the closing process of the various CMS structures thus providing a starting geometry. The precision of these measurements – from 300 μm to about 1 mm – depends on the size of the measured object and the reference system used (local references or nominal global reference system). Due to the sizable motions and deformations of the big structures induced by magnetic forces once the magnet is energized, these survey measurements are no longer a valid representation of the geometry of the detector during operation.

Care must be taken when comparing photogrammetry measurements, which are made with an open detector, to alignment measurements, which are made after detector closing and before any magnet cycles that can cause permanent movements and deformations of large structures. Such measurements are not always directly comparable, since individual measurements might be biased by residual deformations caused by detector lowering (from the surface to the underground cavern), magnetic and gravitational forces, and internal deformations during closing, or thermal effects. In the cross-check and validation tests, all comparisons are done independently for each structure, since detector components (e.g. muon chambers) within a given structure are considered more stable under field-induced deformations. For instance, in the case of the barrel spectrometer, the central barrel wheel is generally used as a reference because it is expected to be the most stable structure in CMS. Under these conditions, it is assumed that, on average, the photogrammetry values and the reconstructed values must agree. Under this assumption and in the absence of systematic biases in the reconstruction, the distribution of the difference between photogrammetry and reconstructed positions is expected to have a mean of zero. The deviation from zero is taken as an estimate of the systematic error in the reconstruction.

Similarly, until a precise track-based validation is available, the precision of the system is given by the standard error propagation of the geometry reconstruction software, which can be checked from residual distributions of laser hits with the corresponding pull distributions.

The complete alignment system for the muon spectrometer of the CMS detector was commissioned at full magnetic field in 2008 during an extended cosmic ray run. The system succeeded in tracking muon detector movements of up to 18 mm and rotations of several milliradians under magnetic forces. Depending on coordinate and subsystem, the optical system achieved chamber alignment precisions of 140–350 μm and 30–200 μrad [32]. Systematic errors on displacements were estimated to be 340–590 μm, based on comparisons with independent photogrammetry measurements.

As mentioned previously, the CMS silicon tracker was aligned using more than 3 million cosmic ray charged particles, with additional information from optical surveys. The positions of the modules were determined with respect to cosmic ray trajectories to a precision of 3–4 μm RMS in the barrel and 3–14 μm RMS in the endcap, in the most sensitive coordinate. The results were validated by several methods, and correlated systematic effects have been investigated. The track parameter resolutions obtained with this alignment are close to the design performance.

For ATLAS the operational experience can be summarized as follows: before each chamber or bar was installed on its support structure, alignment sensors were mounted on it and their proper functioning was verified. The sensors inside chambers and bars, in-plane and in-bar RASNIKs, and temperature sensors were measured. Those measurements were used by ARAMyS to reconstruct the shapes of the chambers and bars. After completing the installation of bars and chambers in a sector or wheel, all alignment sensors were read out. Electronically malfunctioning components were identified, and replaced, until a stable running system was reached. At this point, many or most alignment sensors had partner devices installed, and thus their measurements could be used to obtain from ARAMyS reconstructed chamber and bar positions, which were compared to results from surveys.

At the level of individual MDT sectors, most alignment sensors linking the chambers to the bar worked immediately, that is they acquired valid BCAM or RASNIK images. After the assembly of entire wheels, a recurrent observation was that many azimuthal lines were obstructed, while most or all of the other sensors worked fine. The floppiness of the Big Wheel support structures in this coordinate made this a problem particularly for those wheels: up to 30% of all azimuthal lines in a wheel were initially blocked. The remaining lines were, however, sufficient to reconstruct the positions of all chambers in the wheels to better than a millimeter. This was perfectly adequate for the alignment system to provide the data for repositioning the affected chambers. After repositioning, all of the azimuthal lines were clear. The immediate operation of the alignment system was an essential feature that allowed proper installation of the muon measurement system.

ARAMyS can also be used to simulate the expected performance of an alignment system design based on the foreseen network of sensors and their expected resolutions. For this application, the sensor readout values from a setup are replaced by the expected measurements as calculated by ARAMyS, which are randomly distributed by an amount that reflects the intrinsic resolution and the accuracy of the mounts of individual sensor. The alignment is then reconstructed by using these simulated measurements. A figure of merit is computed from the difference between true and reconstructed chamber positions. For the ATLAS muon spectrometer, the figure of merit is the width of the false sagitta distribution (the false sagitta is the reconstructed deviation from straightness of a straight track traversing a triplet of MDT chambers). As shown on Fig. 32, the ARAMyS simulation predicts a mildly position-dependent false sagitta width in the range of 30–55 μm over the full endcap, well in line with the specifications.

5. Summary and acknowledgements

The alignment systems of large experiments have characteristics that require detailed attention to the design and construction of the entire experiment. The alignment systems are not completely functional while the system is being constructed; the lines of sight are completed only when all components are assembled and in proper position. In CMS, the magnet must be completely closed before all the optical paths line up. In ATLAS, the big and small wheels must be in position before the sensors in the polar lines can see each other. Since many optical “stay clear” paths can be compromised in various ways, measurement systems, structural components, cables and other services, access walkways, and safety equipment all can interfere with the needs of the alignment system. Once these interferences are designed into the system, it is very difficult to correct or work around these problems. Therefore, when doing alignment, it is important to be involved in the detailed layout of the entire detector and to follow

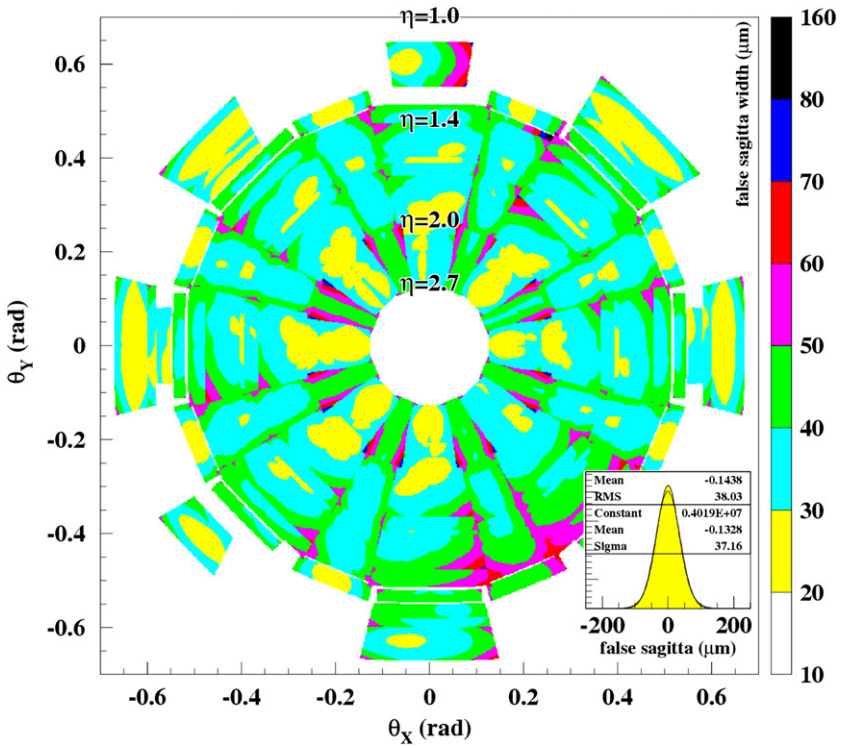

Fig. 32. The sagitta error contribution from the alignment system for the ALTAS endcap chambers. This is determined by simulation using the location and resolution of each of the sensors and mounts in the alignment system.

the evolution of the design and execution throughout the construction of the detector.

Visual inspection on a regular basis is as necessary as following the overall design. Holes left for optical lines offer tempting opportunities for stringing cables or gas lines. Optical lines often are at odd angles, which means that people working on other systems in the detector can be unaware of or have difficulty visualizing the locations of the stay-clear regions and can inadvertently interfere. Detectors are large and dense with equipment, avoiding these errors requires continual vigilance.

Achieving the desired accuracy with the alignment systems generally involves a very large number of small corrections. With small corrections even the sign of the correction is uncertain. There are thousands of sensors in the alignment system; each one will have a set of calibration constants that describes the variation of the sensor from nominal operation. In addition, each detector unit will have its own set of constants. The overwhelming majority of these constants will be small. Errors in any of these constants, since there are so many of them, will have only a small effect on the overall alignment, and thus will be very difficult to identify. Errors in a number of these constants, even though they cannot be identified individually, can have a cumulative effect of degrading the quality of the detector alignment. A maximal effort to maintain quality control at every step in the process of designing and building the alignment system is essential.

At an early stage, a complete and accurate simulation program must be developed to ensure that the proposed design achieves the goals of the system. In particular, due to the complexity of having so large a number of sensors, potential hidden correlations may not be apparent initially. As the design of the detector and requirements of the alignment system evolve, modification of the program can be made to ensure that the integrity of the design can be maintained. Further, as knowledge of the actual behavior of the sensors becomes known, this information can be incorporated into the program to make sure the system maintains its design parameters. Having such a tool is an essential asset in developing the alignment system.

The choice of sensors and sensor mounts is the next important consideration. Because of the many sensors in the detector, simplicity both in design and operation is important. Sensors will have to work for many years and, in many cases, will be difficult to access. Designs must be simple, robust, and not need maintenance. Both CMS and ATLAS independently selected three-point straight-line monitors and CCD cameras for their basic sensor type. These are highly reliable and easy to use. The resolution of the CCD cameras depends on only the mechanical properties of the components. The precision of the CCDs depends on only the layout of the pixels on the silicon; it does not drift or require recalibration.

As important as the sensor is the sensor mount. This device connects the coordinates of the sensor with measurement precision of the tracking detector. Whatever provides the precision of the tracking chamber is often buried inside the chamber, so there must be a clear chain of information connecting the precision of the measurement chamber to the precision of the sensor. The large number of sensors dictates that the mounts and attachment mechanism be simple and robust. The measurement of the mount and the reliability of mounting (and remounting) the sensor can be the limiting factor in the resolution of the alignment system.

Sensor calibration is the set of numbers that relates the sensor mounting mechanics to the precision measurement of the sensor. When the sensor is mounted and read out, the calibration constants of the sensor and the mount allow the sensor reading to determine the location of the tracking chamber. The sensor must be calibrated to sufficient accuracy, as determined by the simulation program, to meet the experimental requirements. For example, the CCD cameras in the ATLAS muon system, called BCAMs, are calibrated so that a distant point of light can be determined to 50 μrad relative to the location of the device to which the camera is attached. Again, the number of sensors

involved suggest that the calibration system be robust and reliable, and in general the simpler the better.

Once the basic concept of the alignment system and technology for the sensors has been chosen, a series of tests have to be performed to insure that the devices and the overall design operate as expected. Of particular importance is a full-scale system test. Although the sensors may be intrinsically simple, the overall design is complex and may have unexpected interactions or anomalies. Operating a partial system that contains all the components in their correct geometric relationship and the full data acquisition chain is critically important. In addition, there should be an external figure of merit, such as a particle beam or particle simulator, to quantify the performance. This should be done for an extended period of time and under a variety of conditions to ensure infrequent errors are uncovered.

The installation and commissioning of the whole detector is another critical issue that should be monitored carefully. As problems or unexpected events in detector assembly arise, decisions have to be made quickly for work-arounds or changes. It is important for the alignment group to be engaged in the process of assembling the detector at every stage to ensure that changes do not cause deterioration the alignment system in a manner that would be difficult or impossible to reverse later. Continuous monitoring of the construction is particularly important, since different parts of the alignment system become operational at different stages of detector completion. Some parts may not become operational until the detector is essentially complete.

Large modern detectors are generally deep underground, with a temperature-stabilized environment and stable running conditions. Structures that hold tracking devices are generally rigid and reliable. For this reason, rapid cycling of the alignment system is not necessary. Usually from once an hour to a few times a day is a sufficient cycle period. But long-term drifts must to be monitored, as do condition changes such as magnet cycling or power cycling from which the detector may not return to the exact same conditions. At these times alignment parameters may have to be updated more frequently.

Many internal checks on alignment systems that can be made, such as χ^2 values of fit results where realistic numbers are used for sensor and component errors or pull distributions of sensor parameters. These validate the system only to the extent that the fundamental design is correct, but do not account for problems or correlations that may have been overlooked. For this reason, external validation is necessary. This can be done by comparison to survey results. Other possibilities are tracking studies, which could include cosmic ray or collision data with magnets on or off, tracks from narrow resonances such as J/ψ's or Z_0's, comparing the behavior of positive and negative tracks, etc. However done, these studies can help identify errors in the system, if any, and give confidence in the validity the final result.

Although generally made of simple devices and sensors used in straightforward ways, alignment systems, often have thousands of parts in an intricate network and with a complex analysis. Many steps are involved in putting together a successful alignment system for large modern detectors. For the project to succeed each step has to be done, carefully and correctly.

To cope with the demanding operational conditions of the LHC accelerator, LHC detectors are characterized by built-in robustness and redundant measurement systems. From this context that emerged the idea of the large and complex optical alignment systems described in this article. Although alignment was included in the initial conceptual designs of the experiments, in the almost 15 years that separated initial concepts from final detector assembly, the specifications and layouts have evolved to adapt to the real detector geometries. During this time, several specific devices were prototyped, developed and implemented in a variety of contexts. The LHC detectors were operational from 2008 are operational and recent 2010 data analysis shows their performance are close to their designs. The effect of alignment in those data is still small due to the current limited statistics. The challenge, for the optical systems, to demonstrate its effectiveness accuracy and precision is still pending as of this writing and will be a case example for future and more demanding machines.

The authors wish to acknowledge the hard work and dedication of all our colleagues, too numerous to list, who share this long and passionate period. The achievements described here would not have been possible without them. In addition we wish to thank the CERN Survey Group, Technical and Integration Teams, and tracking and muon communities of ATLAS and CMS.

References

[1] ATLAS Collaboration, The ATLAS experiment at the CERN large hadron collider, JINST 3 (2008) S08003.
[2] CMS Collaboration, The CMS experiment at the CERN LHC, JINST 3 (2008) S08004.
[3] Three years of digital photogrammetry at CERN, in: Proceedings of the 6th International, Workshop on Accelerator Alignment, Grenoble France October 18–21, 1999, 〈http://www.slac.stanford.edu/econf/C9910183/papers/034.PDF〉.
[4] Proceedings of the First LHC Detector Alignment Workshop. CERN, Geneva, Switzerland 4–6 September 2006; CERN–2007–004 20 June 2007.
[5] Submitted to Eur. Phys. J. C and ATL-COM-Phys-2010-402, 〈http://www.slac.stanford.edu/spires/find/hep/www?eprint=arXiv:1004.5293〉.
[6] The CMS Collaboration, Alignment of the CMS silicon tracker during commissioning with cosmic rays, CMS PAPER CFT-09-003, arXiv:0910.2505v1 [physics.ins-det] 14 October 2009.
[7] H. Dekker, et al., The RASNIK/CCD 3-dimensional alignment system, in: Proceedings of the 3rd International Workshop on Accelerator Alignment, Annecy France, September 28–October 1 1993, 〈http://www.slac.stanford.edu/econf/C930928/papers/017.pdf〉.
[8] Photogrammetry is a commercially available photographic system for locating specialized coded targets in space, We used AICON 3D Studio 5.0.
[9] C. Guyot, et al., The alignment system of the barrel part of the ATLAS muon spectrometer, ATLAS Note, ATL-COM-MUON-2008-002.
[10] S. Aefsky, et al., The optical alignment system of the ATLAS muon spectrometer endcaps, JINST 3 (2008) P11005.
[11] C. Amelung, A. Schricker, Calibration of alignment bars for the ATLAS muon spectrometer endcap, ATLAS Note, ATL-MUON-2005-009.
[12] CMS collaboration, The CMS muon project, Technical Design Report, CERN-LHCC-97-032, 〈http://cdsweb.cern.ch/record/343814〉.
[13] CMS Collaboration, Aligning the CMS muon chambers with the muon alignment system, JINST 5 (2010) T03019.
[14] G. Szekely, et al., Muon barrel alignment system based on a net of PC/104 board computers, in: Proceedings of the 9th Workshop on Electronics for LHC Experiments, Amsterdam The Netherlands, 2003, CERN-2003-006, 〈http://cdsweb.cern.ch/record/722098〉.
[15] P. Arce, Object oriented software for simulation and reconstruction of big alignment systems, in: Proceedings of 7th International Workshop on Accelerator Alignment (IWAA), Spring-8, Japan, 2002.
[16] A. Lopez Virto, Caracterizacion y Pruebas de Validacion Del Sistema Link de Alineamiento de CMS, Ph.D. Thesis, Universidad de Cantabria, Spain, 2003.
[17] J. Dupraz, et al., Nucl. Instr. and Meth. A 388 (1997) 173.
[18] D. Daniels, K. Hashemi, J. Bensinger, BCAM calibration, ATLAS Note, ATL-MUON-2000-026.
[19] W. Blum, et al., Nucl. Instr. and Meth. A 367 (1995) 413.
[20] C. Kohler, et al., Nucl. Instr. and Meth. A 608 (2009) 55.
[21] J. Moromisato, et al., Nucl. Instr. and Meth. A 538 (2005) 234.
[22] W. Wallraff, et al., The AMS infrared tracker alignment system, in: Proceedings of Como 2001, World Scientific.
[23] CMS collaboration, The CMS tracker system project: technical design report, CERN-LHCC-98-006, 〈http://cdsweb.cern.ch/record/368412〉.
[24] CMS collaboration, The CMS tracker: addendum to the technical design report, CERN-LHCC-2000-016, 〈http://cdsweb.cern.ch/record/490194〉.
[25] J. Alberdi, et al., Nucl. Instr. and Meth. A 593 (2008) 608.
[26] M. Hohlmann, et al., Design and performance of the alignment system for the CMS muon endcaps, in: Proceedings of the IEEE Nuclear Science Symposium 2006, San Diego, USA, CR-2008-016, 2008.
[27] A.F. Fox-Murphy, D.F. Howell, R.B. Nickerson, A.R. Weidberg, Nucl. Instr. and Meth. A 383 (1996) 229.
[28] P.A. Coe, An Investigation of Frequency Scanning Interferometry for the Alignment of the ATLAS Semiconductor Tracker, D.Phil. Thesis, Oxford UK, 2001.

[29] S.M. Gibson, et al., A study of geodetic grids for the continuous, quasi real time alignment of the ATLAS semiconductor tracker, In: Proceedings of theSeventh International Workshop on Accelerator Alignment, SPRING8, Japan, November 2002.
[30] M. Sobron, CMS detector geometry reconstructed with the link alignment system, Ph.D. Thesis, Instituto de Física de Cantabria, CSIC-Universidad de Cantabria, 2009.
[31] F. James, M. Roos, Comput. Phys. Commun. 10 (1975) 343.
[32] CMS Collaboration, Alignment of the CMS muon system with tracks from cosmic rays and Beam–Halo muons, JINST 5 (2010) T03020.
[33] The CMS Tracker Collaboration, Alignment of the CMS silicon strip tracker during stand alone commissioning, JINST, vol. 4 (2009) T07001, arXiv:0904.1220. doi:10.1088/1748-0221/4/07/T07001.
[34] D. Green(Ed.), At the leading edge, in: The ATLAS and CMS LHC Experiments, World Scientific.